

# Update of Ground Water Conditions in the Big Lost River Valley

February 2022

By Gus Womeldorph

## Introduction

The Idaho Department of Water Resources (IDWR) maintains a ground water level monitoring network in the Big Lost River Valley. The hydrology of the region serves as an important tributary system to the Eastern Snake Plain Aquifer (ESPA), the aquatic backbone of southern Idaho's agricultural industry.

Ground water conditions in the Big Lost River Valley are explored in several reports, including Crosthwaite et al., 1970, Szczepanowski, 1982, and Johnson et al., 1991, and most recently in a presentation by IDWR's Dennis Owsley in 2014 and an IDWR memo by Jennifer Sukow in 2017. IDWR also recently collaborated with the United States Geological Survey (USGS) and the Idaho Geological Survey (IGS) on several hydrologic studies in the area that resulted in multiple publications including a Big Lost River basin hydrogeologic framework report (Zinsser, 2021) and a surface water-ground water interactions report (Dudunake & Zinsser, 2021). A water budget report developed by the IGS is nearly complete and has an anticipated publishing date of February 2022.

The monitoring network has undergone significant expansion in recent years, including the addition of 20 monitoring wells drilled since fall 2019 and the ongoing addition of pressure transducers where applicable.

## Purpose and Scope

The purpose of this report is to provide an update to the status of the Big Lost River Valley Monitoring Network, last updated in 2017 with Jennifer Sukow's memo and in 1982. This report utilizes water level data collected through calendar year 2020.

## Monitoring Network Status

The Big Lost River Valley Monitoring Network consists of 45 wells that are measured by hand on a semi-annual basis by IDWR staff (Figure 1). Hand measurements are typically taken between March 1-April 15 in the spring and October 15-November 30 in the fall. These timeframes typically avoid land access issues in the winter and irrigation pumping in the summer while gathering valuable seasonal information. Hand measurements are taken with a calibrated electric tape. Pressure transducers have been deployed in 34 of the 45 wells, allowing for water levels to be continually recorded at 1-hour or 12-hour intervals throughout the year (Table 1).

A majority of wells monitored in the valley (42 of 45 wells) are located down-valley of Mackay Dam. In the fall of 2019, 20 monitoring wells were drilled and added to the network, including 6 piezometer nests of 3 wells each. There are 35 wells with pressure transducers installed, and one baro-troll to correct for barometric pressure changes. Water level monitoring in the network dates to 1949, but the total record of individual wells varies widely.

Number	Station Name
1	03N 25E 16ACC1
2	03N 26E 03DAA1
3	03N 26E 16ABB1
4-6	03N 27E 06ACD1-3
7	03N 27E 08BCB1
8	03N 27E 19AAB1
9	03N 27E 19ABB1
10	04N 26E 04BBA1
11	04N 26E 09BCA1
12	04N 26E 16ABB1
13	04N 26E 21ABB1
14-16	04N 26E 21ABB2-4
17-19	04N 26E 23CCC1-3
20	04N 26E 26DCD1
21	04N 26E 32CBB1
22	04N 27E 31DBC1
23	05N 25E 11BAA1
24-26	05N 26E 04BDD1-3
27	05N 26E 05DCB1
28	05N 26E 08CAB1
29	05N 26E 23CDA1
30	05N 26E 32DBA1
31	06N 25E 03AAA1
32-34	06N 25E 10CDA1-3
35	06N 25E 11CBC1
36-38	06N 25E 14DAD1-3
39	06N 25E 18ABB1
40	06N 25E 33AAB1
41	07N 23E 02DDA1
42	07N 24E 28DBA1
43	07N 24E 35CCD1
44	08N 22E 05BAA1
45	09N 21E 14BBC1

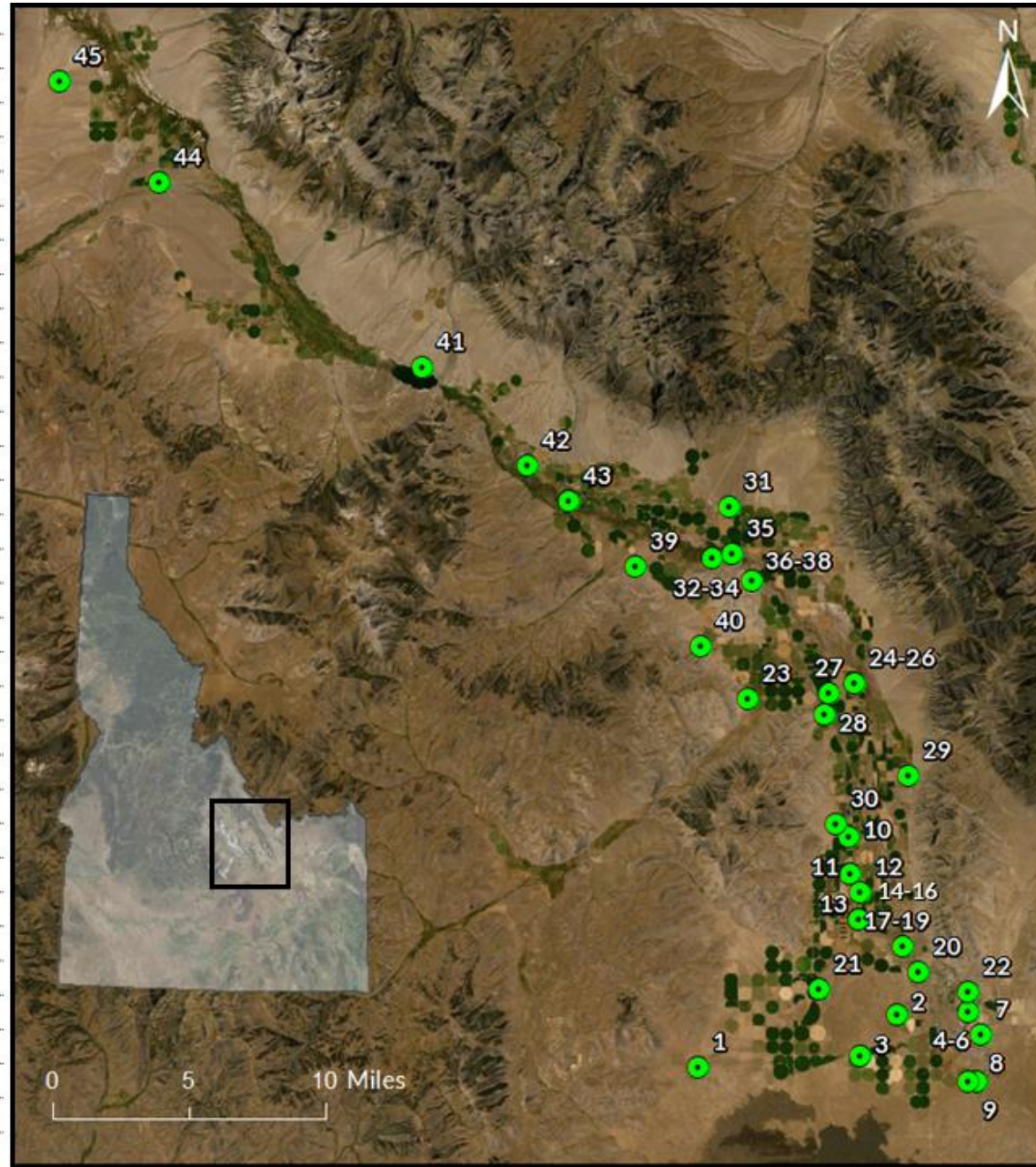


**Figure 1.** Big Lost River Valley Network wells. Semi-annual water level measurements are measured by hand at each well in the spring and fall. Labels with a number range (e.g., 4-6), indicate a piezometer site consisting of three wells.

Table 1: Big Lost River Valley wells monitored by IDWR.

Well Number	Altitude (ft)	Latitude	Longitude	Total Depth (ft)	Opening Min	Opening Max	Period of Record	Transducer
03N 25E 16ACC1	5,530	43.58935	-113.48404	420	320	420	2018-2021	Yes
03N 26E 03DAA1	5,349	43.61637	-113.33769	-	-	-	1967-2021	Yes
03N 26E 16ABB1	5,342	43.59467	-113.36567	580	578	580	2019-2021	Yes
03N 27E 06ACD1	5,298	43.61789	-113.28637	20	10	20	2019-2021	Yes
03N 27E 06ACD2	5,298	43.61784	-113.28637	40	30	40	2019-2021	Yes
03N 27E 06ACD3	5,298	43.61778	-113.28637	60	50	60	2019-2021	Yes
03N 27E 08BCB1	5,274	43.60574	-113.27723	95	-	-	1966-2020	No
03N 27E 19AAB1	5,270	43.58074	-113.28084	240	-	-	1966-2021	No
03N 27E 19ABB1	5,272	43.5802	-113.28611	-	-	-	1980-2021	No
04N 26E 04BBA1	5,444	43.71068	-113.37242	160	55	160	1967-2021	No
04N 26E 09BCA1	5,433	43.69127	-113.37207	96	65	95	2015-2021	Yes
04N 26E 16ABB1	5,409	43.68157	-113.36473	139	36	139	1967-2021	No
04N 26E 21ABB1	5,390	43.66685	-113.36529	760	656	690	1969-2021	Yes
04N 26E 21ABB2	5,393	43.66691	-113.36529	20	10	20	2019-2021	Yes
04N 26E 21ABB3	5,393	43.66696	-113.36529	40	30	40	2019-2021	Yes
04N 26E 21ABB4	5,393	43.66701	-113.36529	60	50	60	2019-2021	Yes
04N 26E 23CCC1	5,356	43.65287	-113.334	20	10	20	2019-2021	Yes
04N 26E 23CCC2	5,356	43.65294	-113.334	40	30	40	2019-2021	Yes
04N 26E 23CCC3	5,356	43.653	-113.334	60	50	60	2019-2021	Yes
04N 26E 26DCD1	5,332	43.63851	-113.32195	143	-	-	1949-2021	Yes
04N 26E 32CBB1	5,371	43.6299	-113.39529	253	206	253	1958-2021	Yes
04N 27E 31DBC1	5,344	43.62824	-113.28612	227	138	227	1949-2021	Yes
05N 25E 11BAA1	5,680	43.78462	-113.44585	220	-	-	1967-2021	No
05N 26E 04BDD1	5,553	43.79255	-113.3673	20	10	20	2019-2021	Yes
05N 26E 04BDD2	5,553	43.79246	-113.36731	40	30	40	2019-2021	Yes
05N 26E 04BDD3	5,553	43.79237	-113.36731	60	50	60	2019-2021	Yes
05N 26E 05DCB1	5,592	43.78685	-113.38585	260	60	260	1967-2021	Yes
05N 26E 08CAB1	5,593	43.77629	-113.38946	202	104	200	1958-2021	Yes
05N 26E 23CDA1	5,488	43.74323	-113.32834	203	-	-	1950-2021	Yes
05N 26E 32DBA1	5,518	43.71796	-113.3814	250	50	245	1978-2021	No
06N 25E 03AAA1	5,770	43.88632	-113.45847	110	-	-	1966-2021	No
06N 25E 10CDA1	5,693	43.85939	-113.47126	20	10	20	2019-2021	Yes
06N 25E 10CDA2	5,693	43.85942	-113.47126	40	30	40	2019-2021	Yes
06N 25E 10CDA3	5,693	43.85946	-113.47126	50	40	50	2019-2021	Yes
06N 25E 11CBC1	5,676	43.86128	-113.45662	160	150	160	2016-2021	Yes
06N 25E 11CBC1BARO	5,676	43.86128	-113.45662	-	-	-		Yes
06N 25E 14DAD1	5,654	43.84712	-113.44227	20	-	-	2019-2021	Yes
06N 25E 14DAD2	5,654	43.8471	-113.44221	40	-	-	2019-2021	Yes
06N 25E 14DAD3	5,654	43.84707	-113.44218	60	-	-	2019-2021	Yes
06N 25E 18ABB1	5,842	43.85533	-113.52763	230	165	230	1967-2021	No
06N 25E 33AAB1	5,810	43.81296	-113.48002	450	-	-	1966-2021	Yes
07N 23E 02DDA1	6,085	43.96144	-113.68308	82	65	80	1967-2021	No
07N 24E 28DBA1	5,888	43.9087	-113.6068	83.5	63	83	1985-2021	Yes
07N 24E 35CCD1	5,837	43.88974	-113.57603	100	-	-	1967-2021	No
08N 22E 05BAA1	6,325	44.05964	-113.87606	87	80	87	1993-2021	Yes
09N 21E 14BBC1	6,386	44.11372	-113.95018	267	167	267	1966-2021	Yes



## Hydrogeology, Geology, and Climate

### Geology and Hydrogeology

The Big Lost River Valley Monitoring Network is located in the Basin and Range province of east-central Idaho, to the north of the Yellowstone-Snake River Plain hotspot. The area is actively extending in the northeast-southwest direction by way of north-northwest-striking normal faults, including the Lost River Fault in the Big Lost River Valley and the Lemhi Fault in the Pahsimeroi and Little Lost River valleys to the east and northeast (Link & Janecke, 1999).

The upper and middle stretches of the Big Lost River Valley are underlain by alluvial sediments up to 2,000 feet thick, representing the main aquifer-bearing units (Crosthwaite, Thomas, & Dyer, 1970). Below Mackay Dam, the valley widens and initiates a complex interaction between surface water and ground water, with the Big Lost River flowing through multiple gaining and losing reaches (Sukow, 2017; Crosthwaite, Thomas, & Dyer, 1970). The Big Lost River disappears completely south of Arco as it becomes underflow to the regional ESPA (Crosthwaite, Thomas, & Dyer, 1970). This represents a major hydrogeological transition from valley fill sediments to the basalt plain characteristic of the ESPA (Sukow, 2017; Owsley, 2014). The transition has important implications on aquifer characteristics, including a downward gradient to the ESPA and the corresponding increase in depth of the water table. Recharge to the ground water system in the Big Lost River Valley comes from losing reaches of the Big Lost River and from tributary streams, infiltration from excess irrigation and irrigation canals, and precipitation (Sukow, 2017; Crosthwaite, Thomas, & Dyer, 1970).

Declining water levels in the Big Lost River Valley have been well documented going back, at least, to Crosthwaite et al., 1970. Such declines have led to an increase in losing reaches in the Big Lost River (Owsley, 2014). In response to falling ground water levels across the ESPA following 6 consecutive years of drought, IDWR ordered a moratorium on April 30, 1992, on the processing and approval of applications for consumptive use of ground water permits (Higginson, 1992). The moratorium extends north to Mackay Dam (Figure 2).

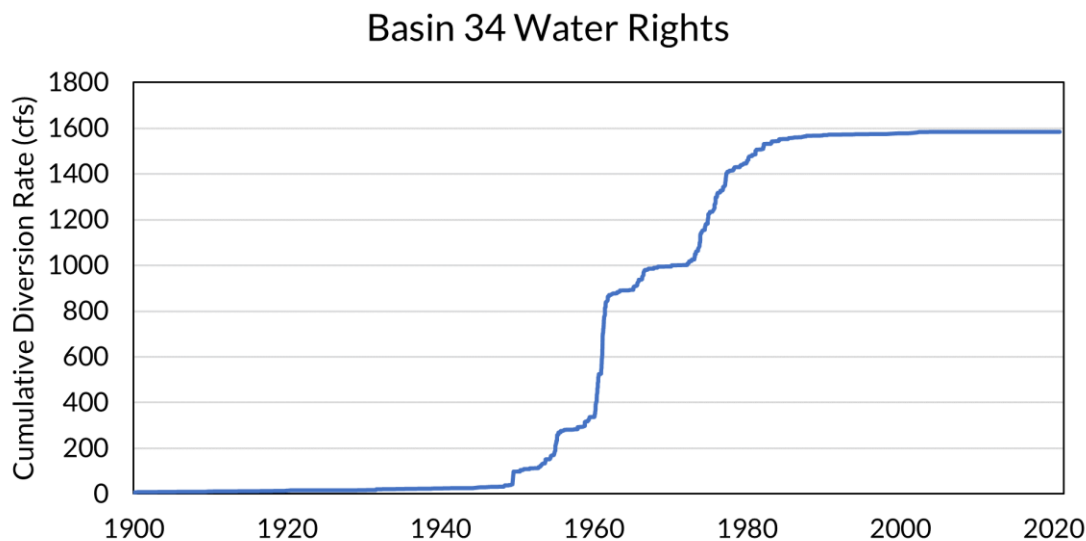


**Figure 2** Cumulative water rights for Basin 34, the watershed including the Big Lost River Valley.

### Palmer Drought Severity Index

The Palmer Drought Severity Index (PDSI) is a tool that uses precipitation and temperature measurements in a physical water-balance model to provide a measure of drought for a given region (Dai, 2019). Correlated to soil moisture content, PDSI provides a useful snapshot of the natural water availability of a region over time (Dai, Trenberth, & Qian, 2004). The output is a unit-less number where more negative values indicate drier conditions and more positive numbers indicate wetter than normal conditions. The Big Lost River Valley Monitoring Network, located down-valley from Copper Basin, is best represented by the climate division for the Idaho Northeastern Valleys region shown in Figure 3 (Dai, 2019). The region is subject to large year-to-year swings in total precipitation, an important observation as the ground water and surface water supply is largely supplied by precipitation from surrounding mountains (Owsley, 2014; Crosthwaite, Thomas, & Dyer, 1970).

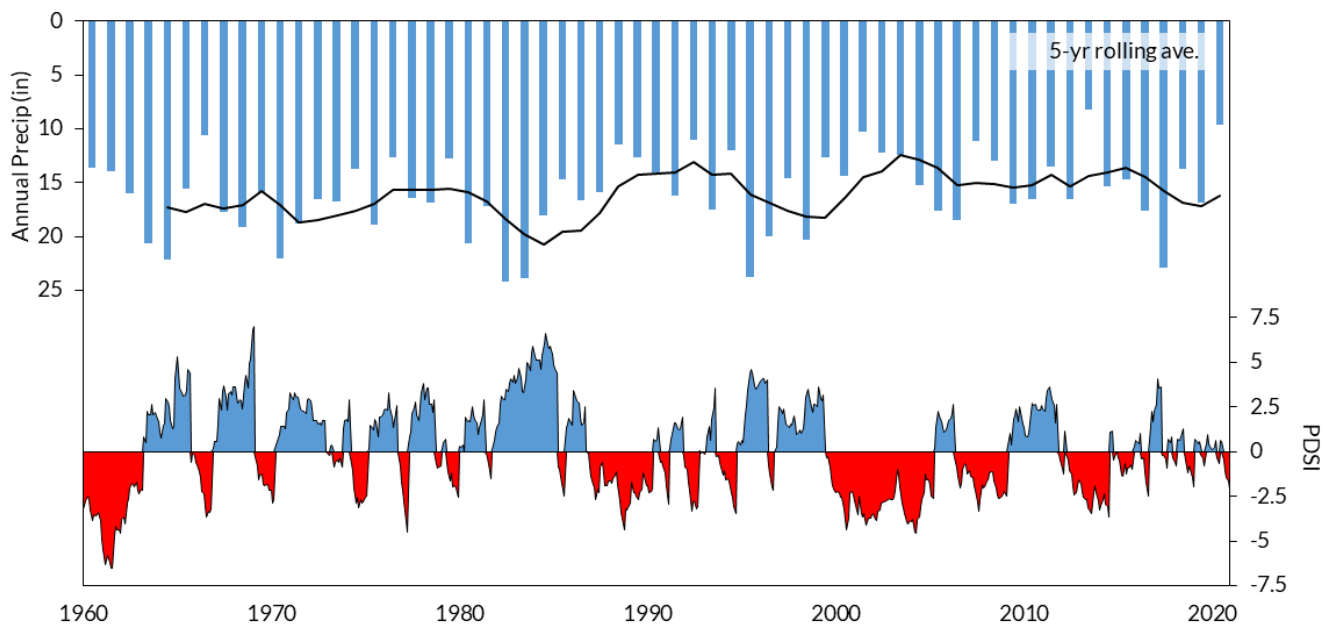


**Figure 3** Palmer Drought Severity Index for Idaho Northeastern Valleys region and annual precipitation totals with 5-year moving average in the Copper Basin, ID.

PDSI conditions for the region are shown in Figure 3 and listed in Table 2, divided into 1960-2020, 1960-1989, and 1990-2020. For the period of 1960-2020, the Big Lost region is in drought condition 25.8% of the time, near normal 48.2% of the time, and wetter than normal the remaining 26% of the time. Division of the PDSI into pre- and post-1990 time periods reveals overall drier conditions for the latter period with a higher percentage of near normal conditions.

**Table 2:** Network PDSI conditions, 1960-2020.

PDSI condition	PDSI value	1960-2020	1960-1989	1990-2020
Extreme Drought	$x \leq -4$	2.9%	4.7%	1.3%
Severe Drought	$-4 < x \leq -3$	8.2%	6.2%	10.2%
Moderate Drought	$-3 < x \leq -2$	14.7%	12.1%	17.5%
Near Normal	$-2 > x > 2$	48.2%	39.7%	54.0%
Unusually Moist	$2 \geq x > 3$	12.7%	16.2%	10.2%
Very Moist	$3 \geq x > 4$	7.4%	10.6%	4.8%
Extremely Moist	$x \geq 4$	5.9%	10.6%	1.9%

## Water Level Analysis

Water levels in the Big Lost River Valley Monitoring Network were analyzed by calculating seasonal water level changes, applying Mann-Kendall trend tests, and comparing water table contours from different years. These methods helped explore long- and short-term water level changes for both individual wells and the region, incorporating new information from well additions where applicable. Hydrographs for the network wells over their entire record are presented in Appendix [A](#).

## Water Level and Precipitation Correlation

Correlating discrete precipitation to ground water levels can yield varying results due to the dependence of the ground water level at a given time and location to the antecedent ground water level, even in ground water systems that are understood to be highly dependent on precipitation (Smail et. al., 2019). Smail (2019) utilizes a cumulative deviation or departure from mean (CDM) to measure antecedent precipitation and correlates it to variations in ground water levels, allowing for a comparison that accounts for the antecedent water level conditions. For the purposes of the Big Lost River Valley Network update, the CDM method from Smail (2019) is used to explore the correlation between water levels at each well with (1) precipitation at each well site and (2) precipitation at the higher elevations of the Copper Basin.

Monthly precipitation values for the Copper Basin and at individual well sites from 1895 through 2021 were downloaded from the Oregon State University PRISM Climate Group data explorer website (PRISM Climate Group, 2021). Following the method developed in Smail (2019), moving mean sequences were calculated at 12-month steps from 12- to 480-month windows. Precipitation deviations from each moving mean window were calculated and used to create a CDM time series for each window at each site. Next, the CDM time series at each site were compared to the water level record using Pearson's correlation coefficient, which calculates the level and direction of covariation of two given variables with a result from -1 to 1, where -1 indicates a perfect negative relationship, 1 indicates a perfect positive relationship, and 0 indicates no relationship (Costa, 2017 as cited in Smail, et. al., 2019). Finally, the moving mean precipitation window with the highest correlation with ground water level was chosen for each well location and across the entire network. Smail (2019) divided correlation results into high ( $>0.5$ ), moderate ( $0.3 - 0.5$ ), and low ( $<0.3$ ), a criterion followed in this analysis.

The optimal moving mean window for Copper Basin precipitation correlations across all sites was 108 months (9 years) at an average Pearson correlation of 0.67, with 17 of the 21 sites (81%) at a high correlation between CDM and water level variation, 2 of the 21 sites (9.5%) at a moderate correlation, and 2 of the 21 sites (9.5%) at a low correlation (Appendix [B](#), Table B.1).

The optimal moving mean window for individual well site precipitation across all sites was 120 months (10 years) at an average Pearson correlation of 0.58, with 13 of the 21 sites (62%) at a high correlation between CDM and water level variation, 4 of the 21 sites (19%) at a moderate correlation, and 4 of the 21 sites (19%) at a low correlation (Appendix B, Table B.1). The optimal moving mean precipitation windows for each site is presented in Appendix B, Table B.2, for both Copper Basin precipitation and individual site precipitation.

The CDM analysis reveals a high correlation between Copper Basin precipitation and network well sites, highlighting the significant effect of precipitation in the upper elevations of the basin to ground water levels throughout the network.

## Water Table Contours

Water table contours for the Big Lost River Valley Monitoring Network were created using the Spline with Barriers tool in ArcGIS 10.6. Fall measurements from as far back as 1967 were used to create the contours to maintain a consistent, representative suite of wells for comparison.

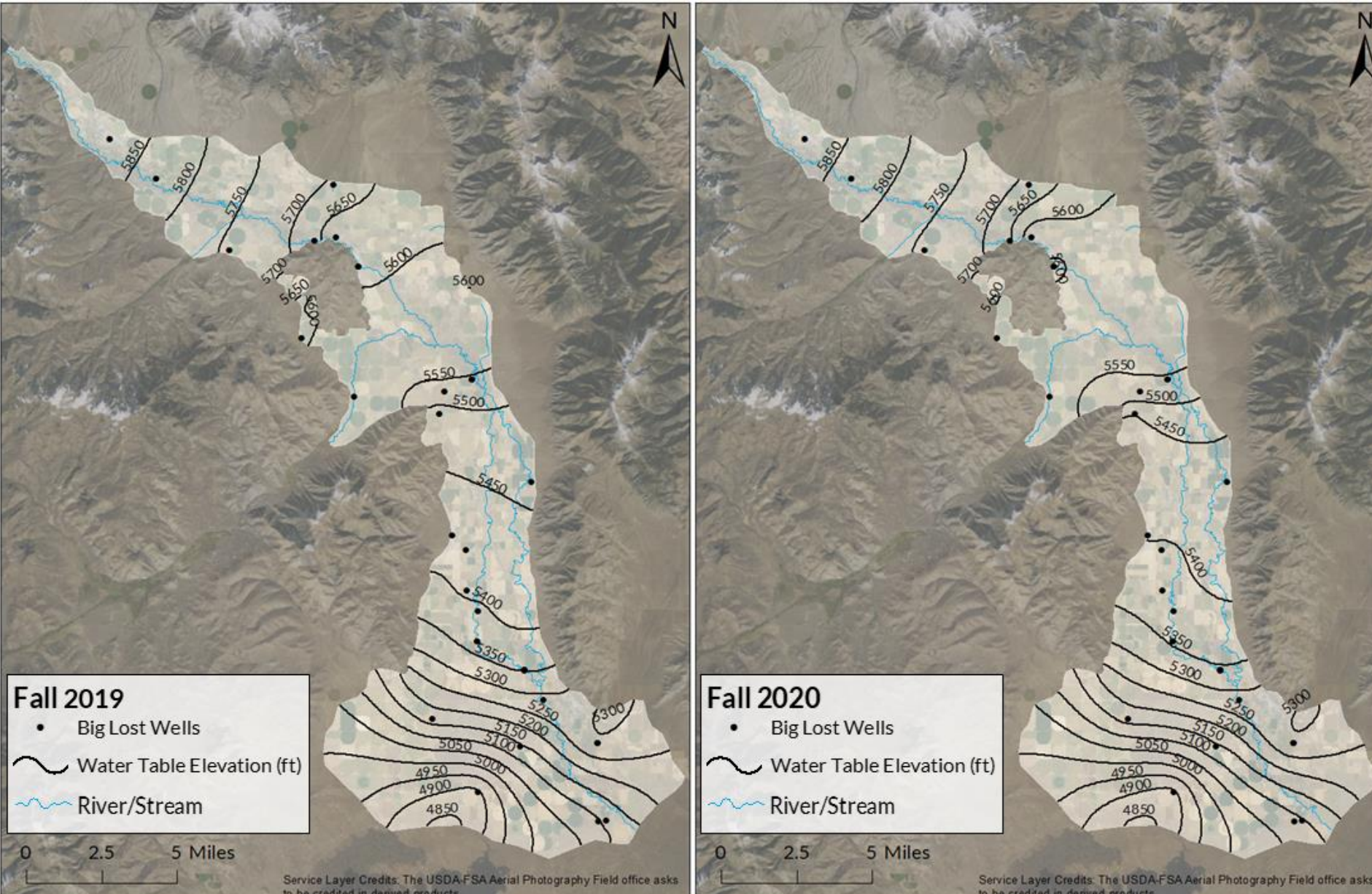
A polygon representing the Big Lost valley aquifer, developed for this report, and extending from Arco to Mackay Dam was used as the water table contour boundary. Water table contours were created and compared for two time periods: fall 1967 versus 2020 and fall 2019 versus 2020.

Figure 4 compares water table contours in the Big Lost River Valley for fall 2019 and 2020 and demonstrates the variability of water table levels in the area from year-to-year. Note how the potentiometric surface lowers and the ground water contours move up-valley in 2020 above elevation 5250, indicating a deepening of the ground water system. Twenty wells were drilled and added to the network in fall of 2019 and are included in these contour maps.

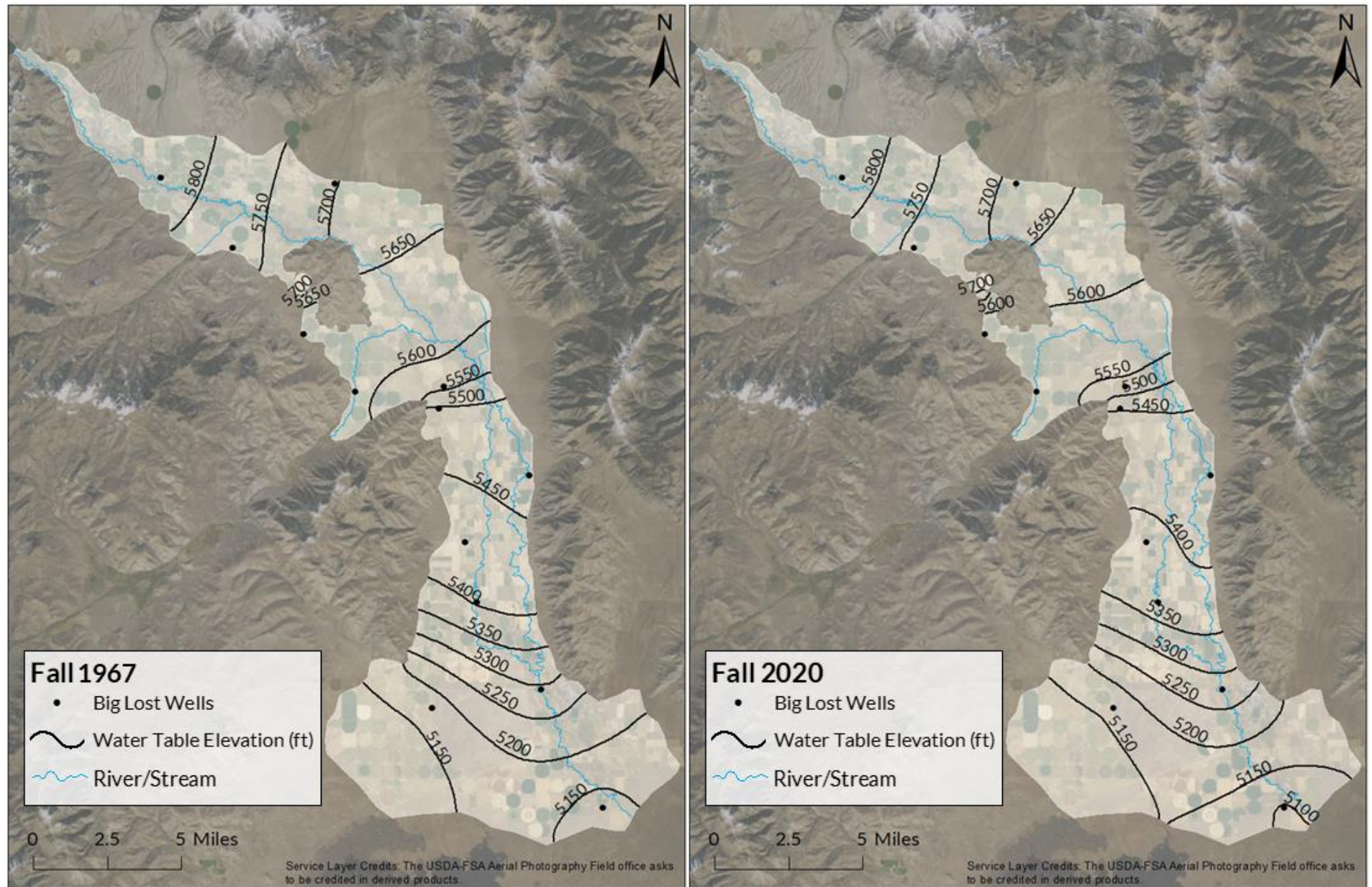
Figure 5 shows water table contours for the Big Lost River Valley in fall 1967 and 2020, with the intent of presenting the water table change as far back as the record for a representative set of wells would allow. The potentiometric surface lowers and ground water contours move up-valley in 2020 versus 1967, again indicating a deepening of the ground water system.

Figure 6 quantifies the deepening of the ground water system and presents the change in water table elevation for the two time periods, 1967 to 2020 and 2019 to 2020. The contours and change maps show significant water level declines across much of the valley, most evident in the central portion of the valley with up to 30 feet of decline from 2019 to 2020 and over 40 feet of decline during the 53-year period from 1967-2020.









**Figure 5** Water table elevation contours for the Big Lost River Valley below Mackay Dam, fall 1967 and fall 2020. Significant declines in water levels for that time period are present in much of the valley, such as the shift of the 5450 ft contour.



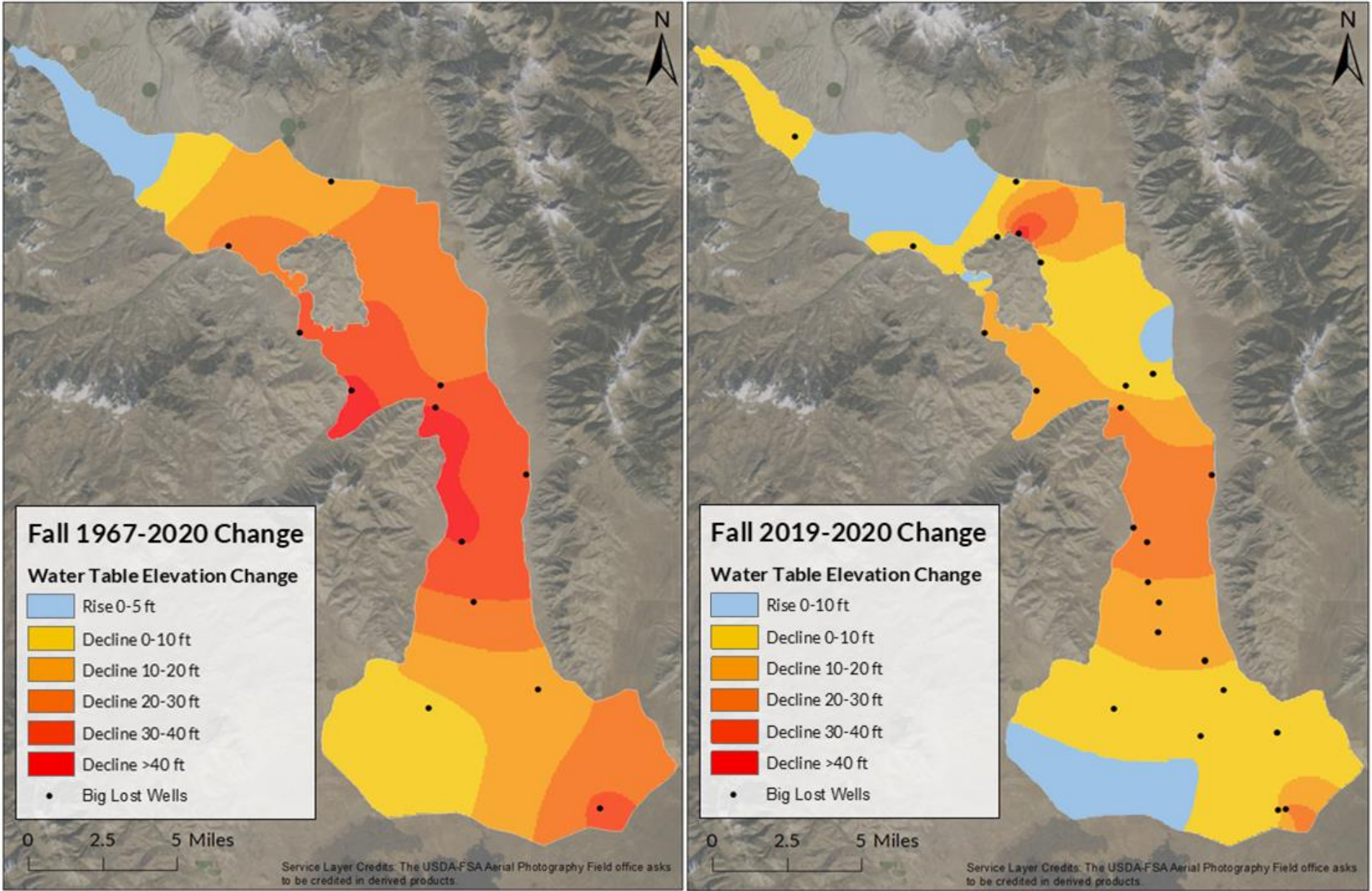


**Figure 6** Water table elevation change in the Big Lost River Valley Network wells, fall 1967-2020 (left) and fall 2019-2020. Large ground water level changes are represented in each change map, indicative of the potential for high variation in water levels over time in the Big Lost River Valley.

Trend Analysis

The Big Lost River Valley Monitoring Network fall water level measurements were used to test for ground water level trends using the Mann-Kendall and Regional Kendall computer program described by Helsel et al., 2006. The Mann-Kendall test describes trend over time while providing a measure of the trend’s statistical significance (Helsel & Hirsch, 2002). The Regional Kendall (RMK) test provides a measure of trend over multiple sampling locations in a region, in this case the Big Lost River Valley (Helsel & Frans, 2006).

Mann-Kendall trend results for the Big Lost River Valley wells over the entire record show statistically significant ( $p<0.05$ ) declines in water levels in 9 of the 45 wells, and a statistically significant rise in one well (Attachment C and Figure 7). The rising trend was observed in 04N 27E 31DBC1, which was completed in limestone, making it unique compared to the other wells in the network. The remainder of the Big Lost River Valley wells resulted in non-significant trend results (Table C.1).

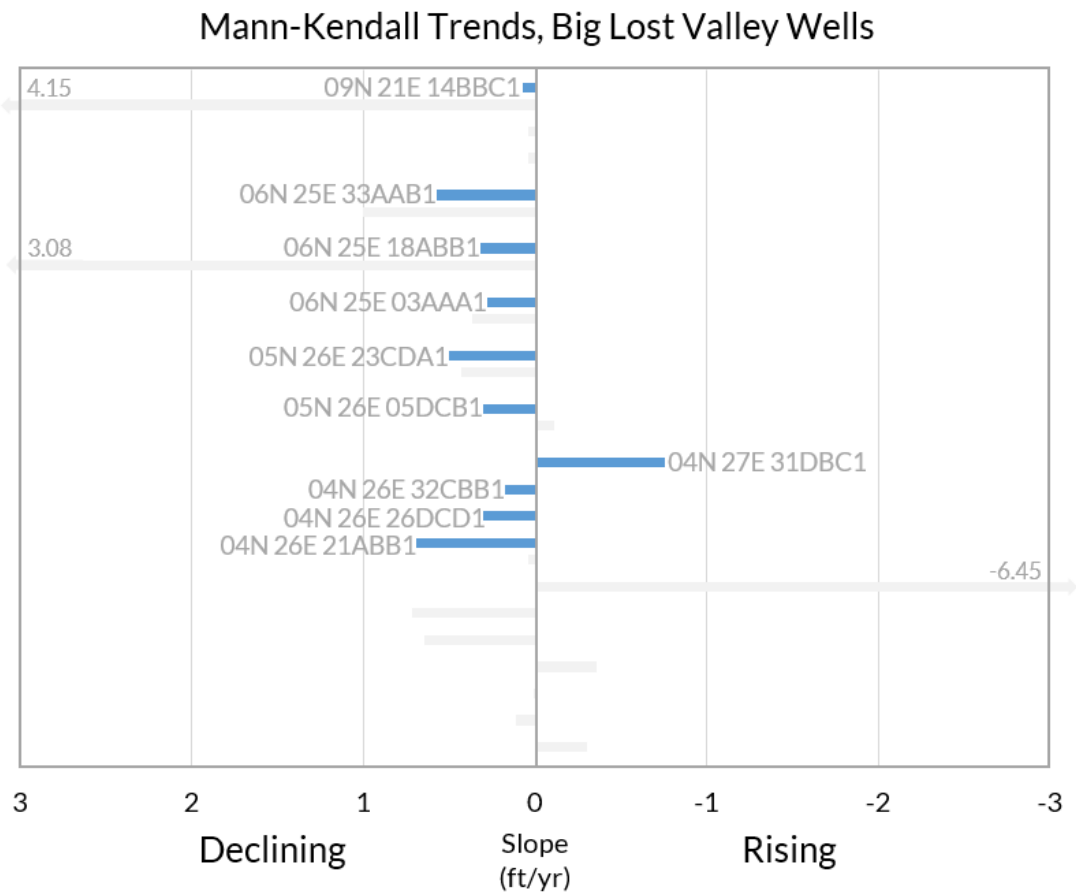


**Figure 7** Mann-Kendall trend results for wells in the Big Lost River Valley. Blue bars represent wells with a significant trend ( $p<0.05$ ), while gray bars show wells without a significant trend ( $p>0.05$ ). Gray numbers exceed the limits of the x-axis. A positive slope indicates a declining water level trend, as depth to water measurements were used.

Regional Kendall trend tests in the Big Lost River Valley Network were performed using three different time periods: 1970-2020, 1990-2020, and 2010-2020 (Table C.2). The 1970-2020 RMK test resulted in a 0.38 ft/yr decline in water levels across the five wells with sufficient data to test. The 1990-2020 RMK test revealed a 0.11 ft/yr decline in water levels across the 12 wells with sufficient data. The 2010-2020 RMK test showed a 0.4 ft/yr rise in water levels across the 19 wells with sufficient data. Each RMK test for the network wells yielded statistically significant results.



## Seasonal Water Level Change

Water level changes from spring to fall were calculated for each well in the Big Lost River Valley Network, including maximum, minimum, and average seasonal changes (Attachment [D](#), Table [D1](#)). The single-well average seasonal changes were then averaged.

The valley-wide average for spring-fall ground water fluctuation in the network is 0.51 feet, when not including the single-year record of the 20 new wells. This indicates a rise in water levels from spring to fall, likely a result of infiltration from irrigation and from river seepage over the growing season.

## Discussion

Water level contours, hydrographs, and trend analysis indicate declining water levels in the Big Lost River Valley over the long-term. The 1967-2020 water level contours and change map reveal water level declines, particularly in the central portion of the valley (Figure [6](#)). Mann-Kendall trends for individual wells show statistically significant water level declines in 9 wells versus a rise in water level for one well, while the Regional Kendall test shows a statistically significant decline of 0.38 ft/yr (Table [C.2](#)).

Short term trends offer a mixed view of water levels in the network. Regional Kendall tests for 1990-2020 and 2010-2020 show a decline of 0.11 ft/yr and a rise of 0.40 ft/yr, respectively. Year-to-year precipitation change, shown in the PDSI analysis for the region (Figure [3](#), Table [2](#)) and reflected in the 2019 to 2020 change map (Figure [6](#)), can result in a significant rise or fall in water levels across the valley in the short term.

While the overall long-term trend of Big Lost River Valley aquifer is declining, the wet years of 2017 and 2018 correlated to rather significant rises in aquifer levels throughout the valley. These changes, in addition to the declining water levels observed during dry years and the high correlation between ground water levels and Copper Basin precipitation revealed by the CDM, illustrate the direct connection between the surface water resources and the underlying aquifer in this valley. The CDM analysis also shows the significance of precipitation in the upper elevations of the basin to ground water levels throughout the network.

## Conclusions and Recommendations

Due to declining long-term ground water levels in the Big Lost River Valley, it is recommended that IDWR continue monitoring on a semi-annual schedule and continue to add wells to the network where possible. The network would benefit from additional wells in several areas of the valley, including north of Mackay Dam and west of the Big Lost River near Mackay. Three new shallow piezometers were drilled in July 2021, near the mouth of Antelope Creek, helping to fill a long-identified data gap. Currently, IDWR is working with the USGS to coordinate a large-scale mass measurement of over 200 wells in the valley, many of which may be candidates for addition to the monitoring network.

## Bibliography

- Climate Prediction Center Internet Team. (2005, 6 15). *Explanation*. Retrieved from National Weather Service Climate Prediction Center:  
[https://www.cpc.ncep.noaa.gov/products/analysis\\_monitoring/cdus/palmer\\_drought/wpdanote.shtml](https://www.cpc.ncep.noaa.gov/products/analysis_monitoring/cdus/palmer_drought/wpdanote.shtml)
- Costa, V. (2017). Correlation and regression. In V. Costa, *Fundamentals of Statistical Hydrology* (pp. 391-440). Springer.
- Crosthwaite, E. G., Thomas, C. A., & Dyer, K. L. (1970). *Water Resources in the Big Lost River Basin, South-Central Idaho*. Boise: US Geological Survey.
- Dai, A. (2019, 12 12). *The Climate Data Guide: Palmer Drought Severity Index (PDSI)*. Retrieved from NCAR, UCAR Climate Data Guide: <https://www1.ncdc.noaa.gov/pub/data/cirs/climdiv/>
- Dai, A., Trenberth, K. E., & Qian, T. (2004). A Global Dataset of Palmer Drought Severity Index for 1870-2002: Relationship with Soil Moisture and Effects of Surface Warming. *Journal of Hydrometeorology*, 1117-1130.
- Dudunake, T. J., & Zinsser, L. M. (2021). *Surface-Water and Groundwater Interactions in the Big Lost River, South-Central Idaho*. Reston: U.S. Geological Survey.
- Helsel, D. R., & Hirsch, R. M. (2002). *Statistical Methods in Water Resources*. United States Geological Survey.
- Helsel, D. R., Mueller, D. K., & Slack, J. R. (2006). Computer program for the Kendall family of trend tests.
- Helsel, D., & Frans, L. (2006). Regional Kendall Test for Trend. *Environmental Science & Technology*, 4066-4073.
- Higginson, R. (1992, May 15). *Snake River Basin Upstream From Weiser Moratorium Order*. Retrieved from idwr.idaho.gov: <https://idwr.idaho.gov/files/legal/orders/1992/19920515-Original-ESRP.pdf>
- Johnson, G., Ralston, D., & Mink, L. (1991). *Ground-Water Pumping Impacts on Surface Water Irrigation Diversions From Big Lost River*. Boise: Idaho Water Resources Research Institute.
- Link, P. K., & Janecke, S. U. (1999). Geology of East-Central Idaho: Geologic Roadlogs for the Big and Little Lost River, Lemhi, and Salmon River Valleys. *Guidebook to the Geology of Eastern Idaho*, 295-334.
- Mundorff, M. J., Broom, H. C., & Kilburn, C. (1963). *Reconnaissance of the Hydrology of the Little Lost River Basin, Idaho*. Washington: US Government Printing Office.
- Owsley, D. (2014, December 10). *Big Lost Aquifer System*. Retrieved from idwr.idaho.gov: <https://idwr.idaho.gov/files/general/20141210-Big-Lost-Aquifer-System.pdf>
- PRISM Climate Group, O. (2021). *Time Series Values for Individual Locations*. Retrieved from <https://prism.oregonstate.edu/explorer/>
- Smail, R., Pruitt, A., Mitchell, P., & Colquhoun, J. (2019). Cumulative deviation from moving mean as a proxy for groundwater level variation in Wisconsin. *Journal of Hydrology X*.

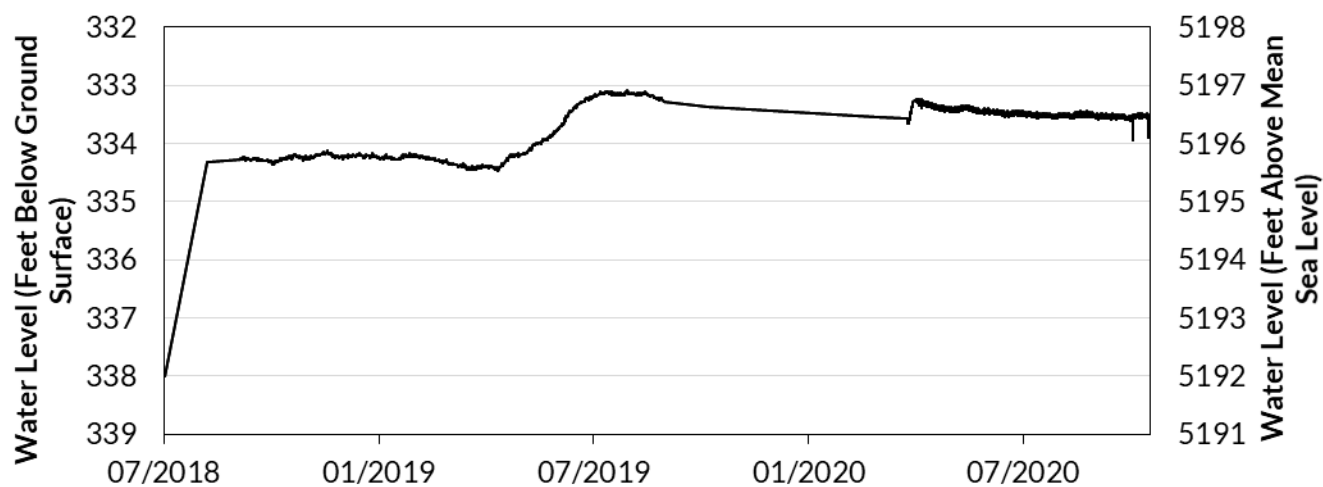
- Sukow, J. (2017, February 6). *IDWR Staff Memo regarding Big Lost River Valley*. Retrieved from idwr.idaho.gov: <https://idwr.idaho.gov/files/legal/p-cgwa-2016-001/p-cgwa-2016-001-20170206-idwr-staff-memo-re-blrv-by-jennifer-sukow.pdf>
- Szczepanowski, S. P. (1982). *Review of Ground-Water Conditions in the Big Lost River Valley*. Boise: Idaho Department of Water Resources.
- Zinsser, L. M. (2021). *Hydrologic Framework of the Big Lost River Basin, South-Central Idaho*. Reston: U.S. Geological Survey.



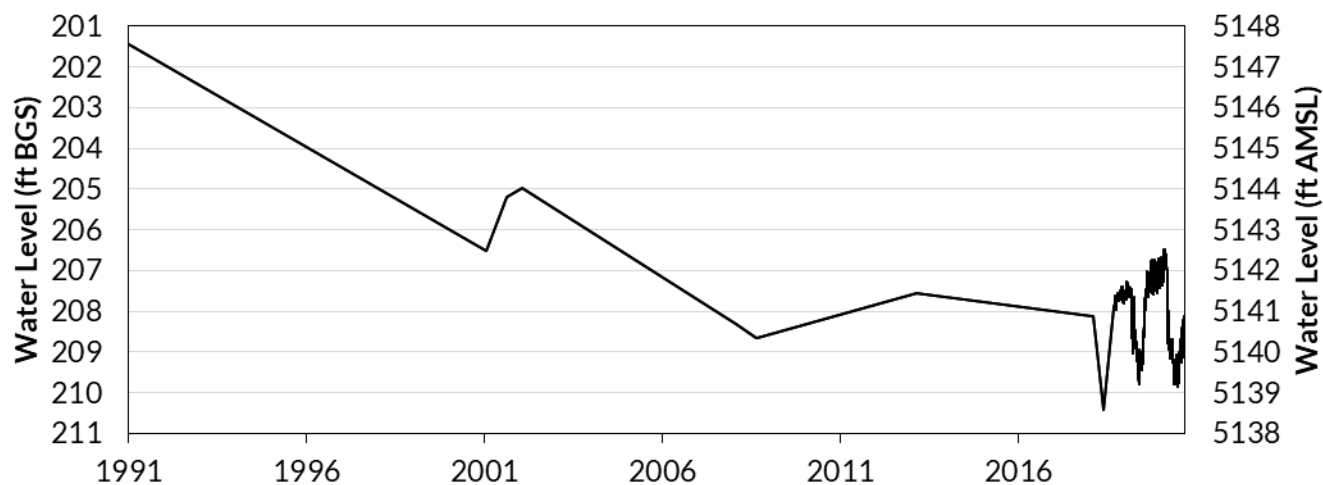
## Appendix A – Hydrographs

Note: Hydrographs are excluded for dry wells: 06N 25E 10CDA1, 06N 25E 10CDA3, and 06N 25E 14DAD1

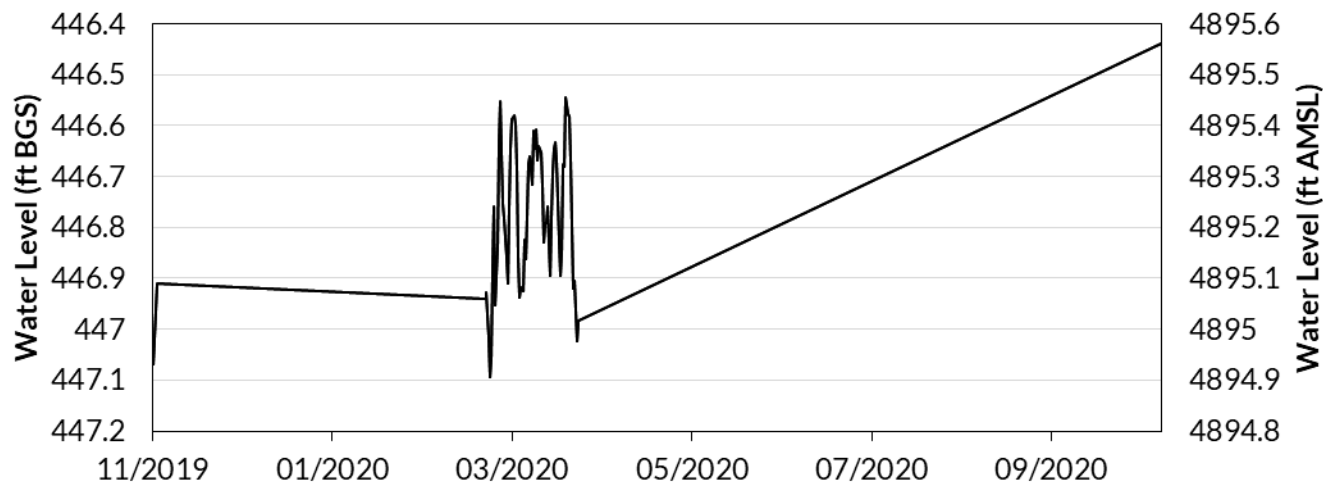
03N 25E 16ACC1

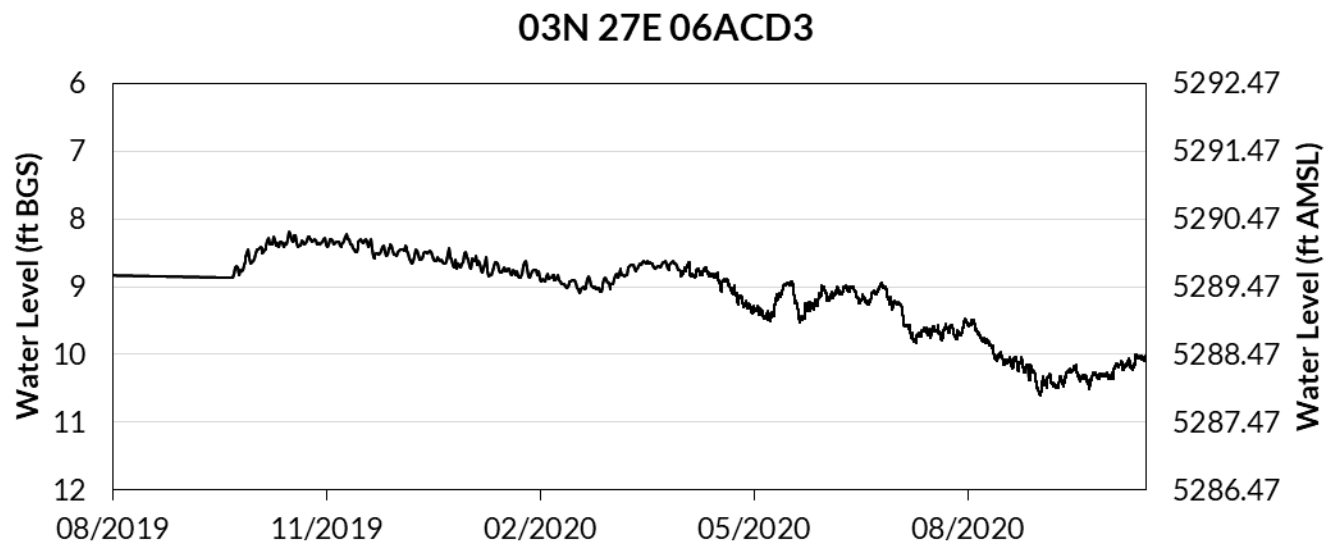
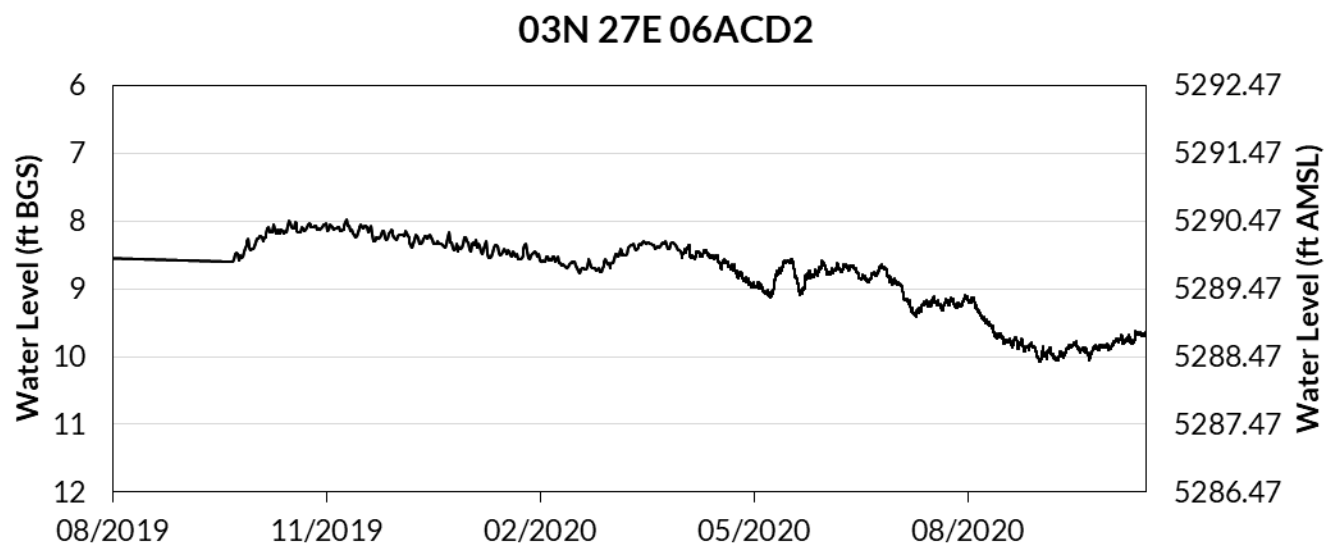
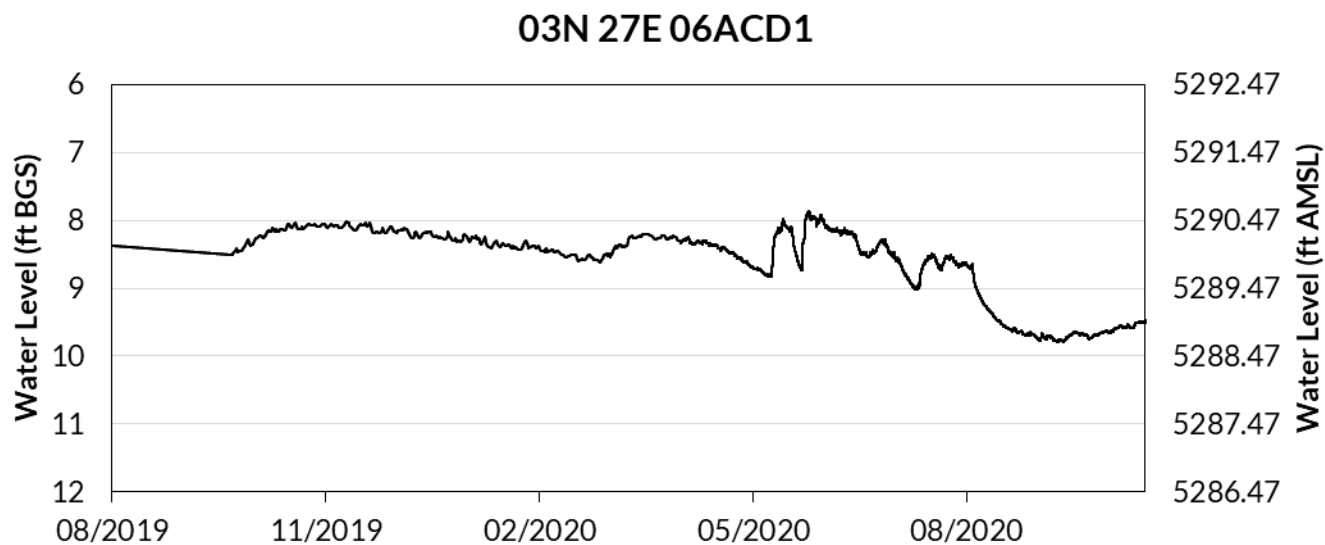


03N 26E 03DAA1

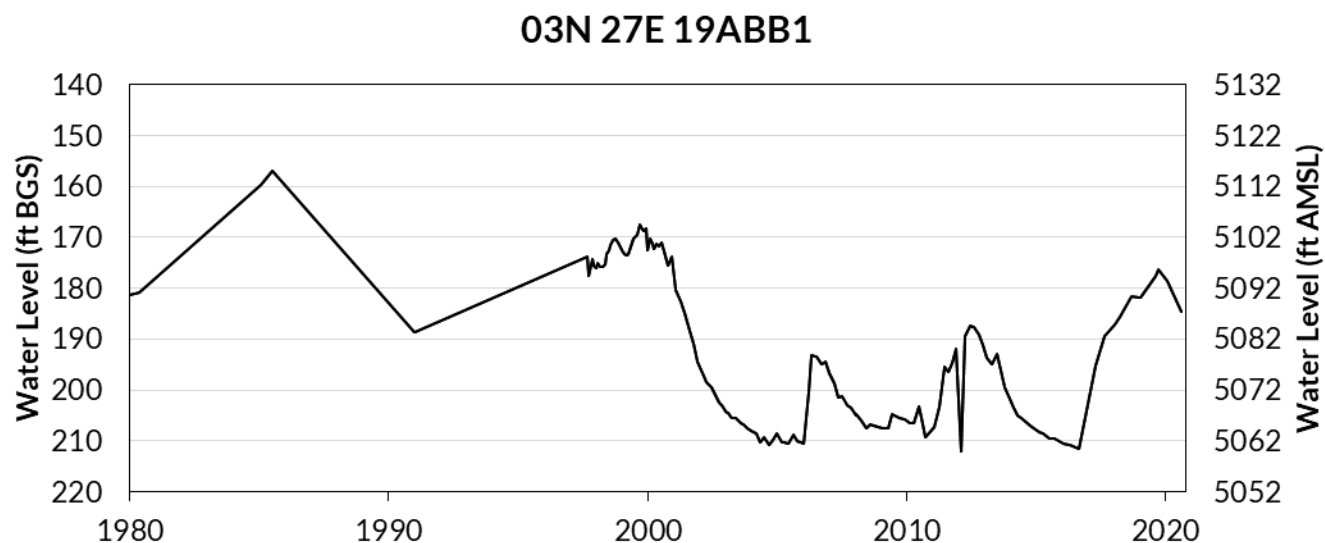
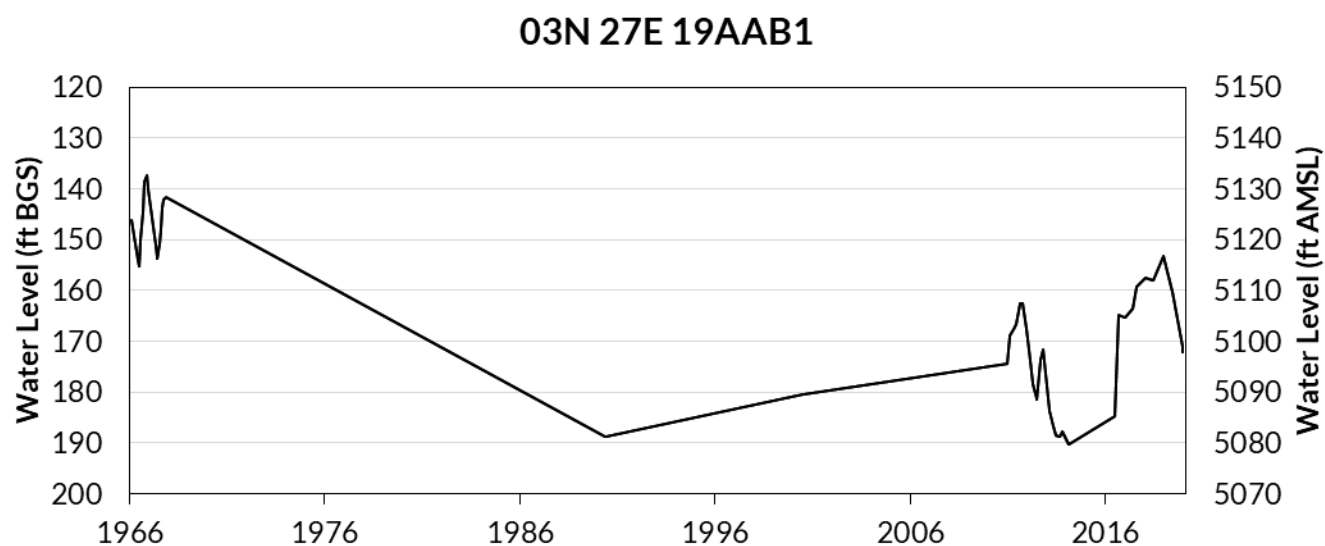
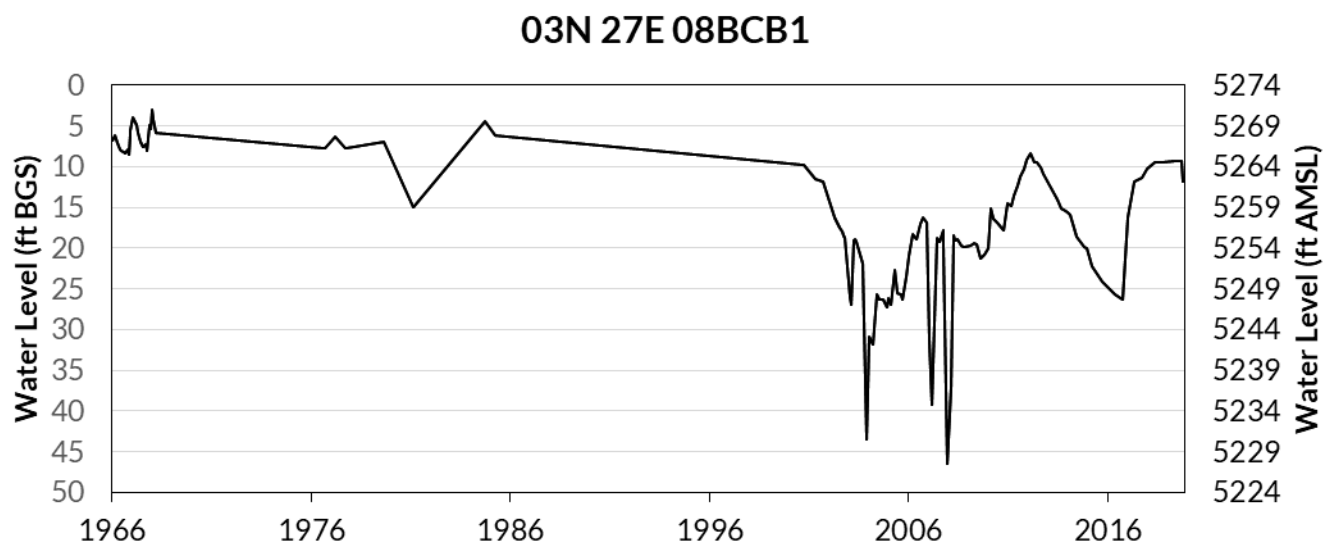


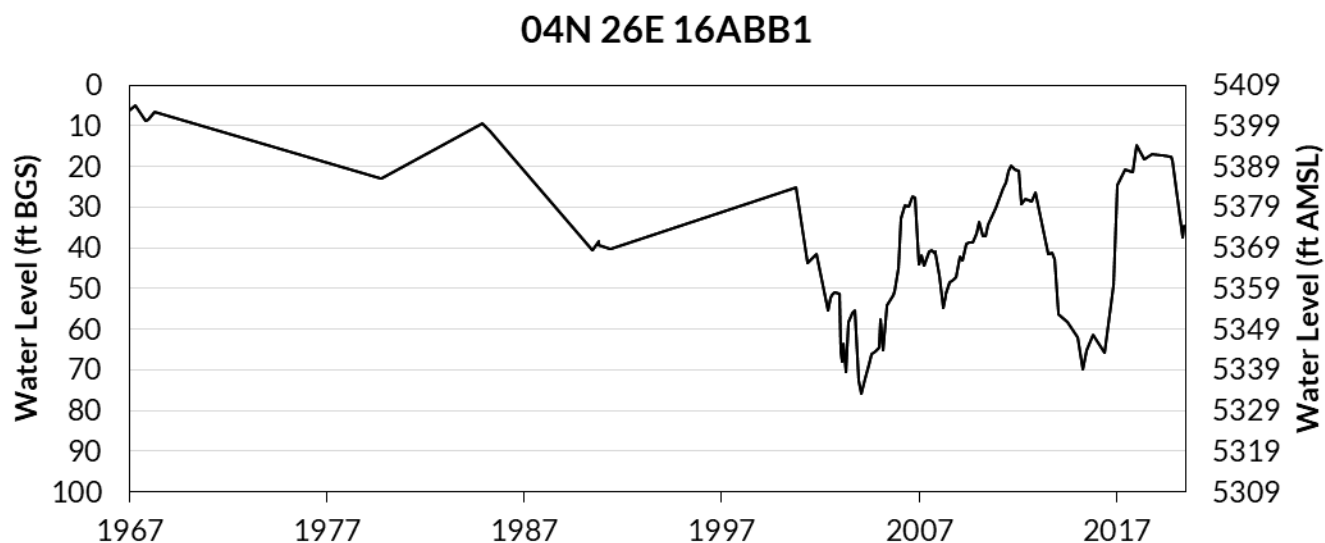
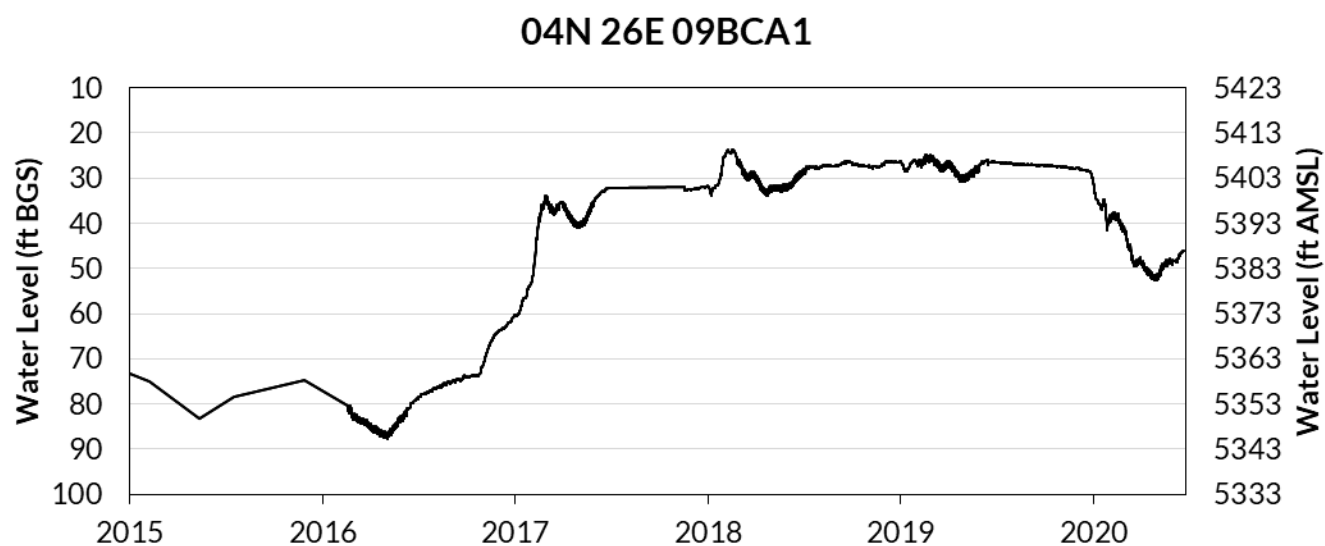
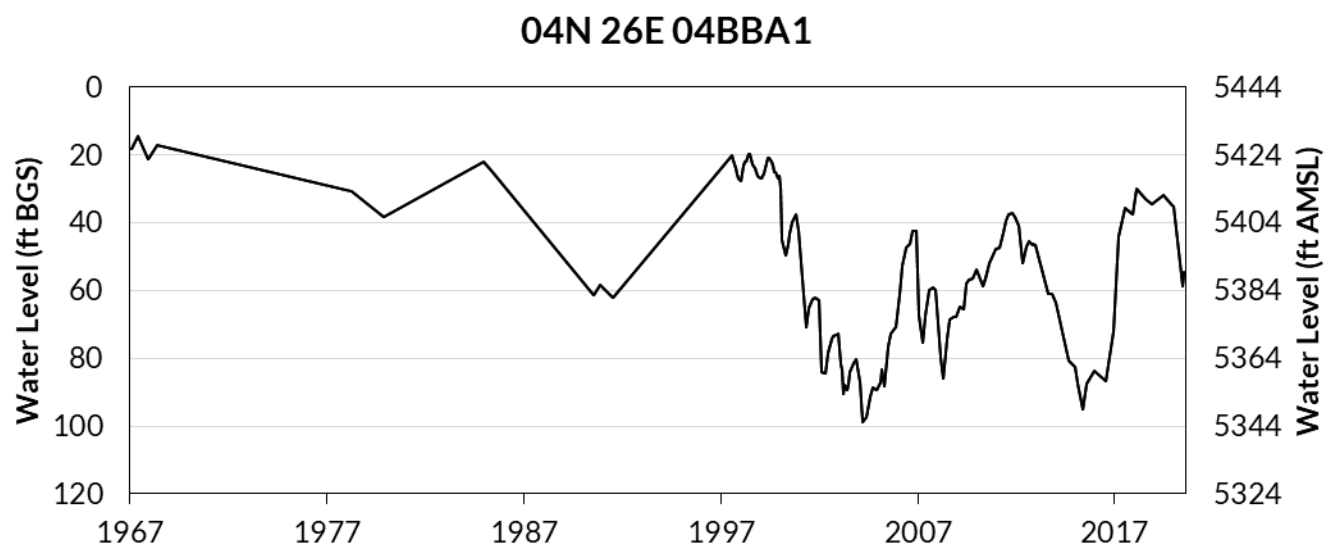
03N 26E 16ABB1



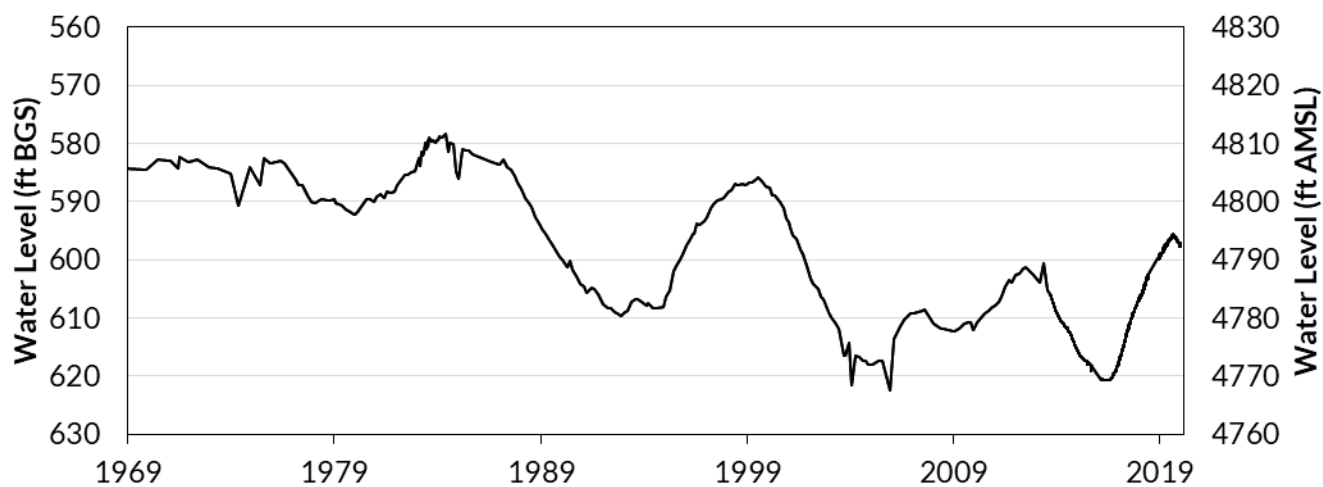




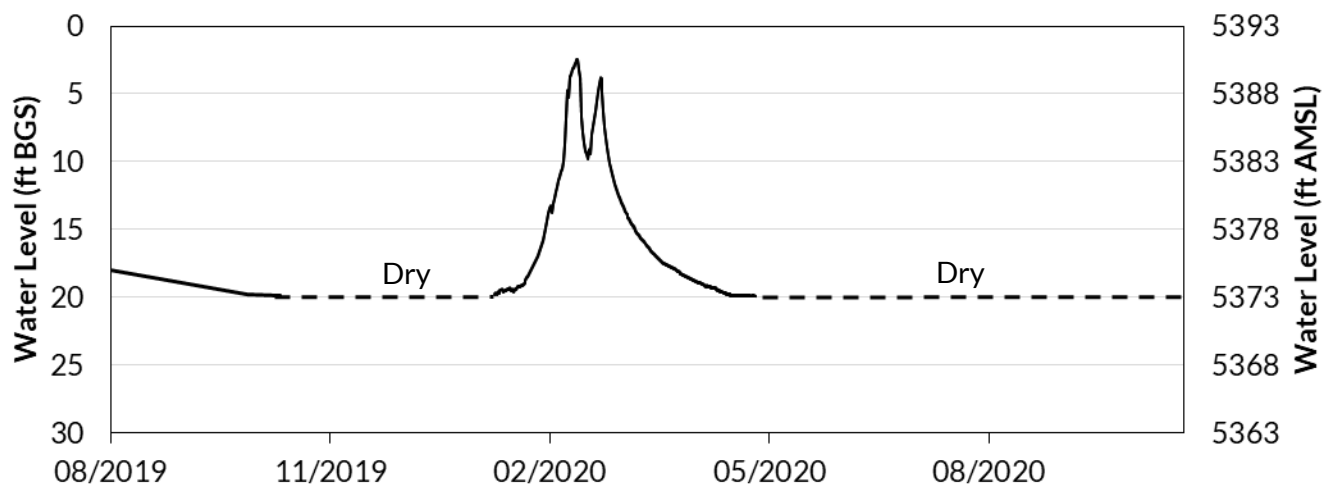




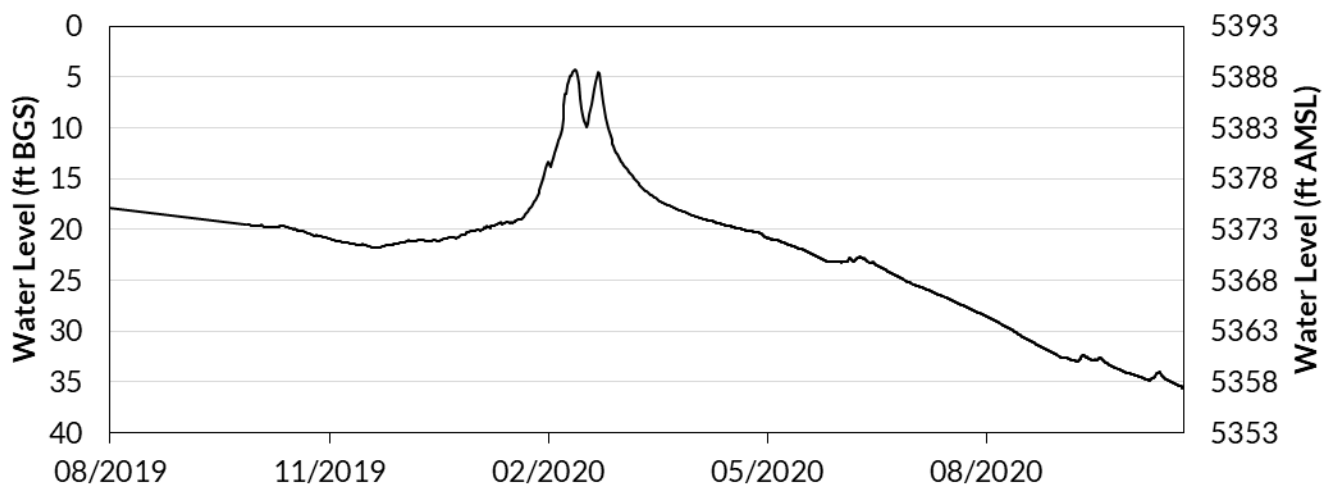
04N 26E 21ABB1



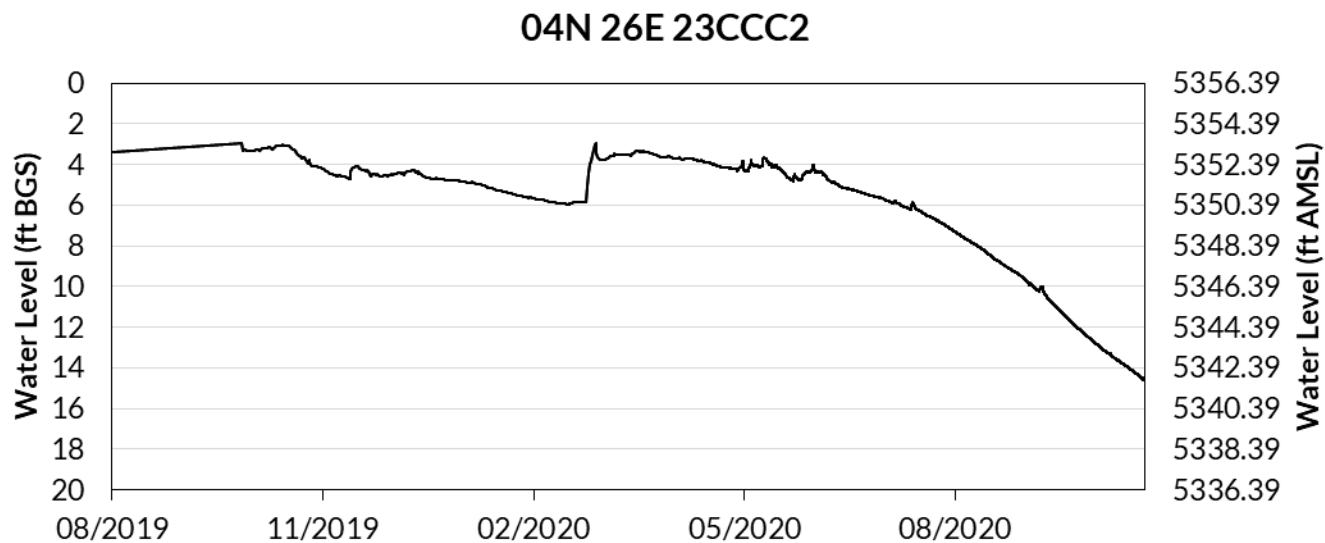
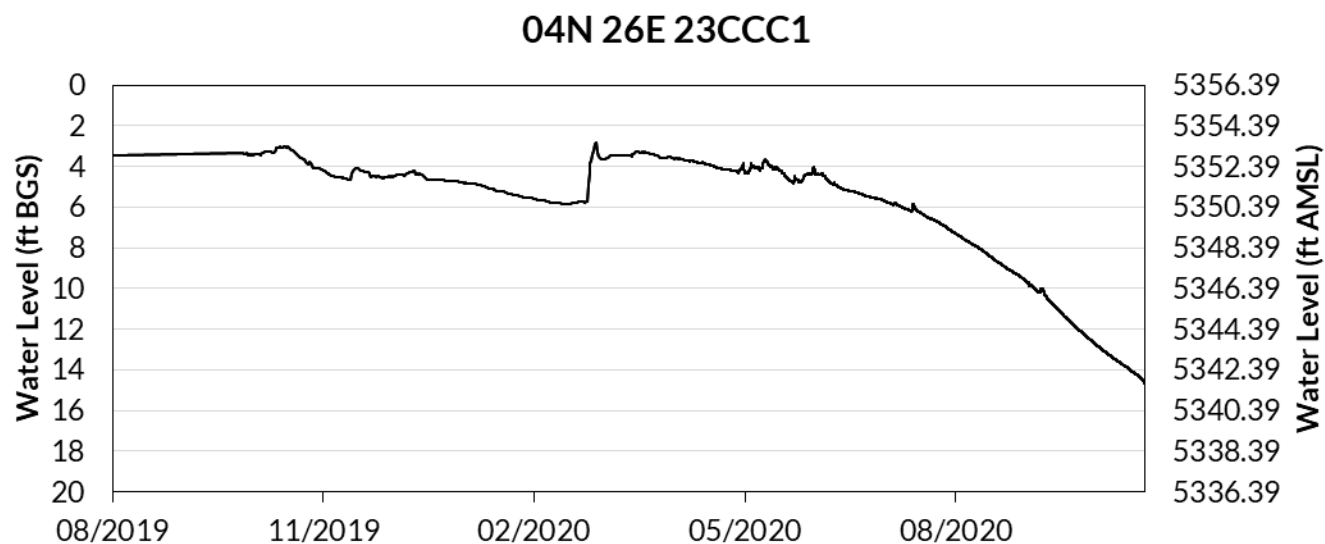
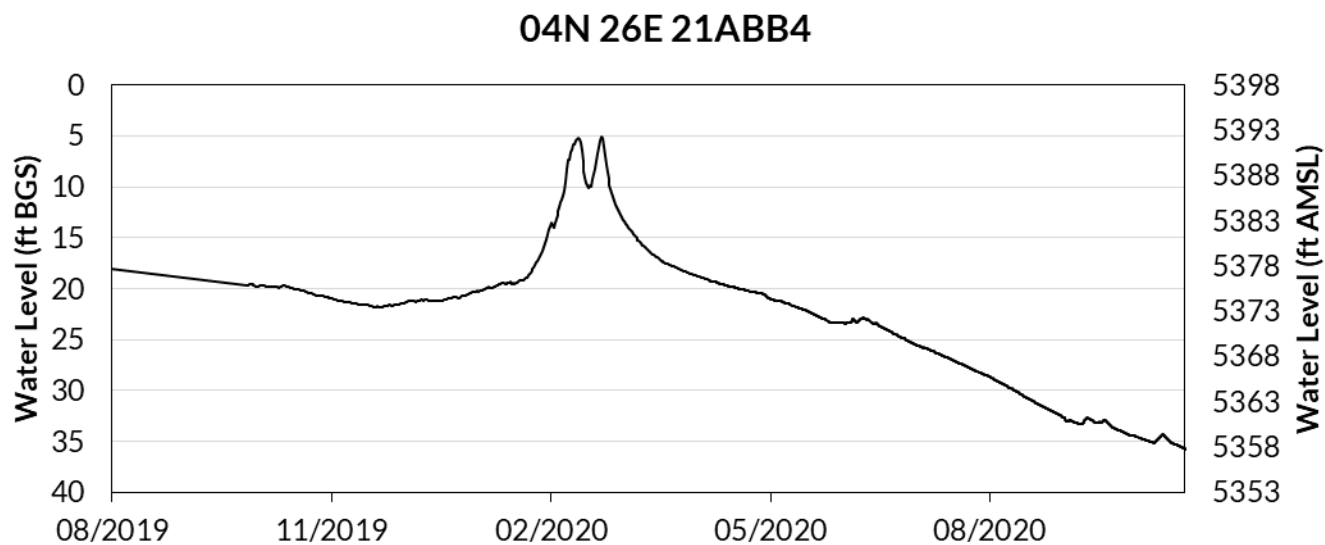
04N 26E 21ABB2

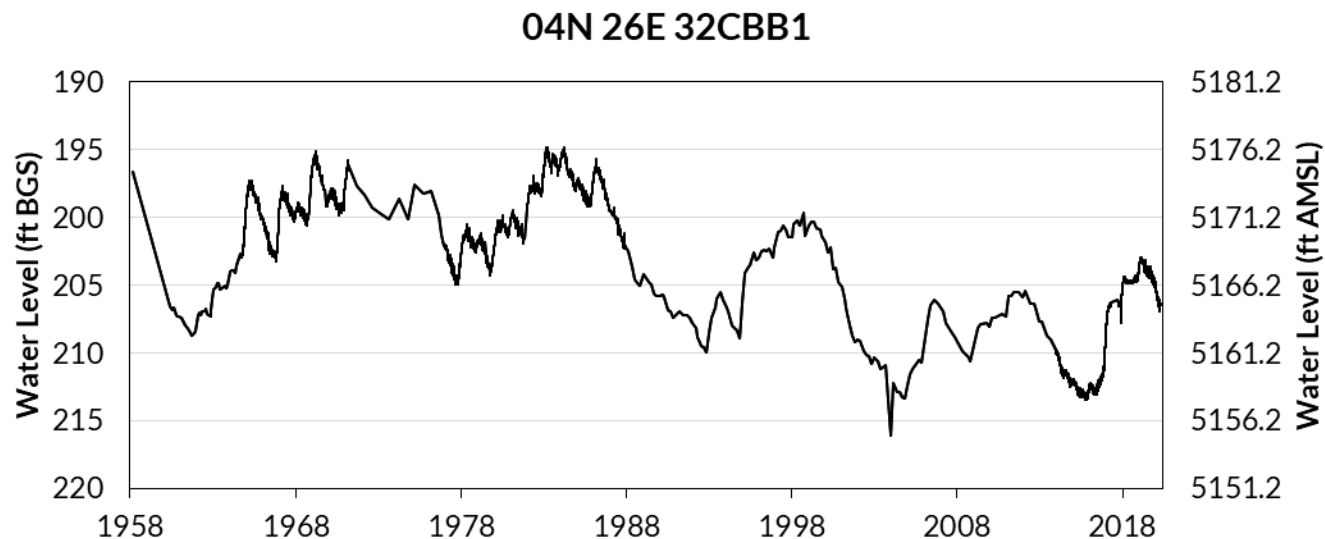
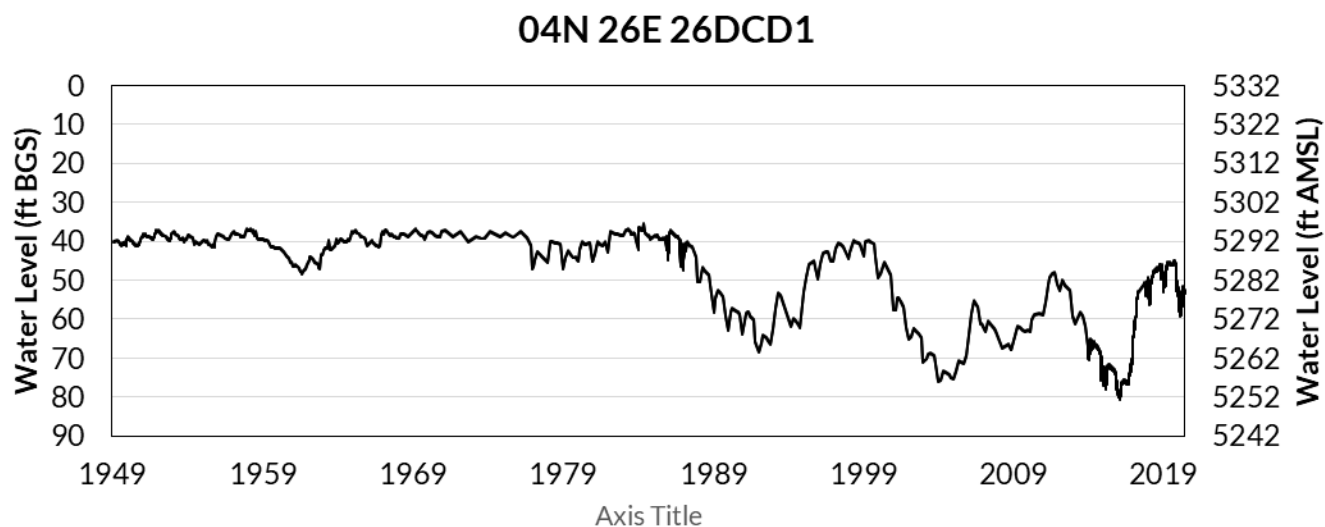
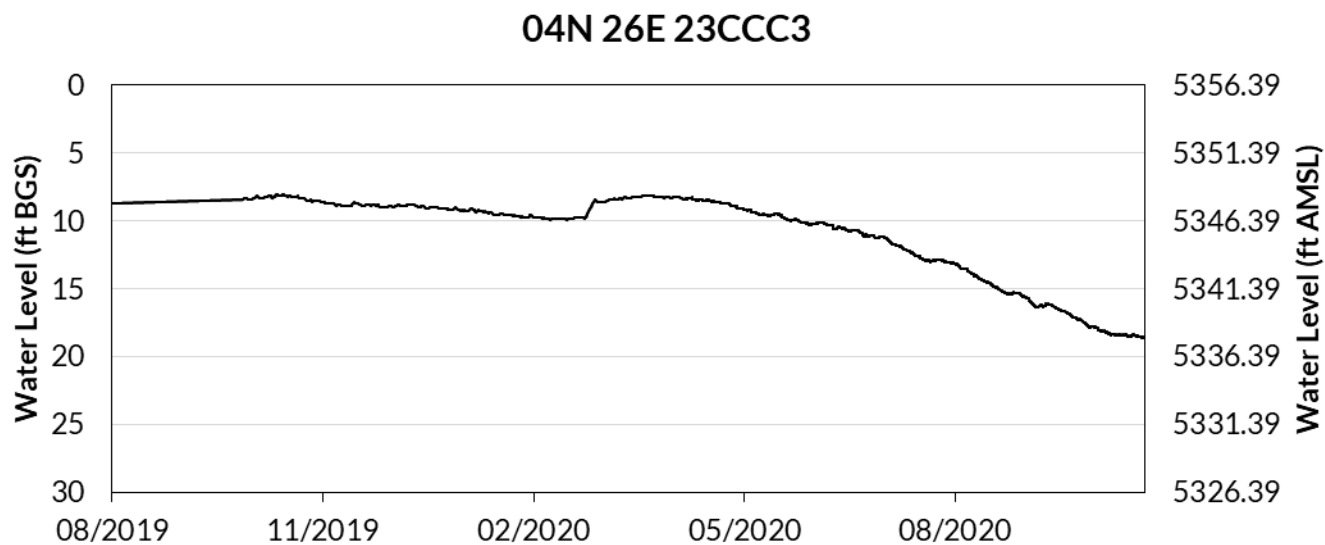


04N 26E 21ABB3





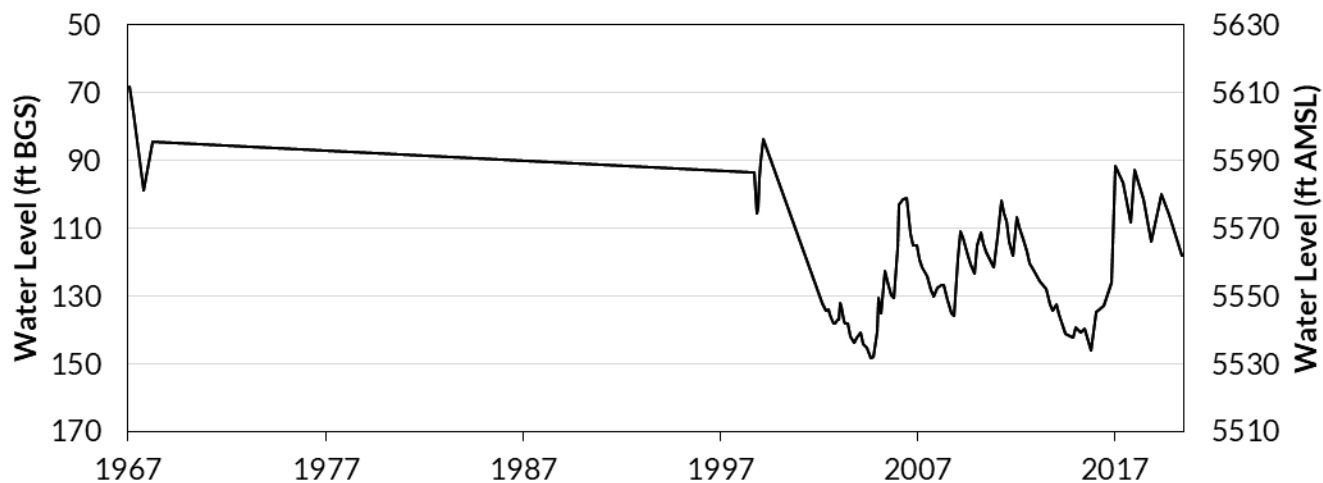




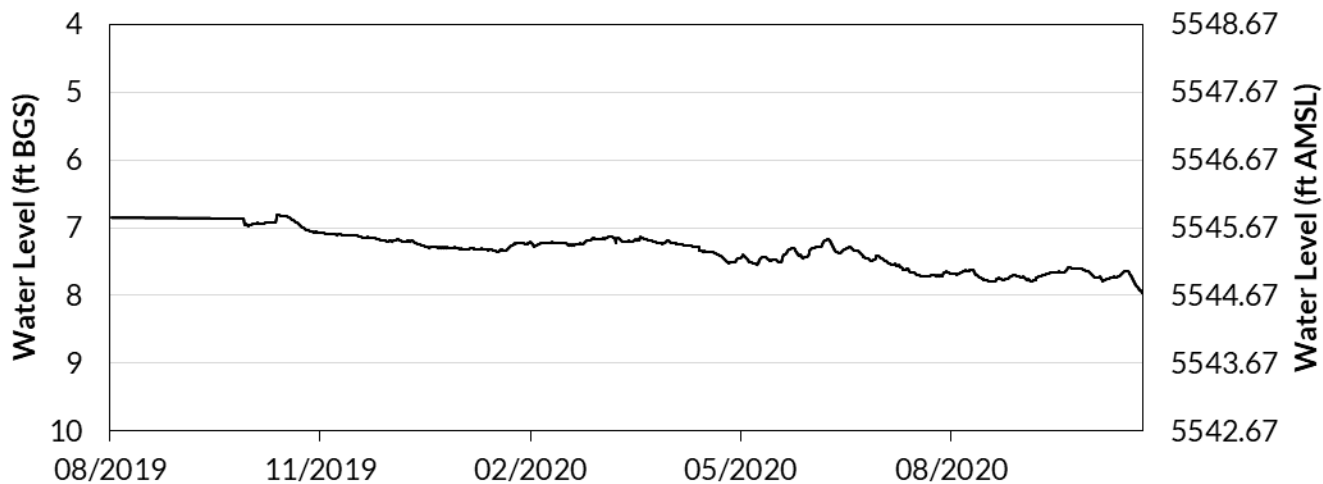
04N 27E 31DBC1



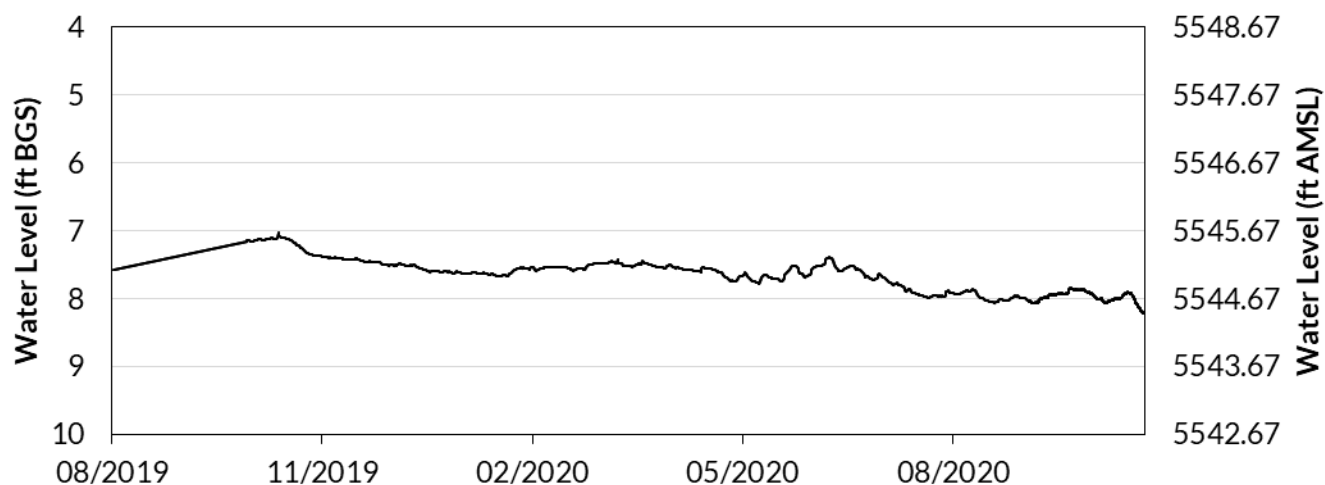
05N 25E 11BAA1



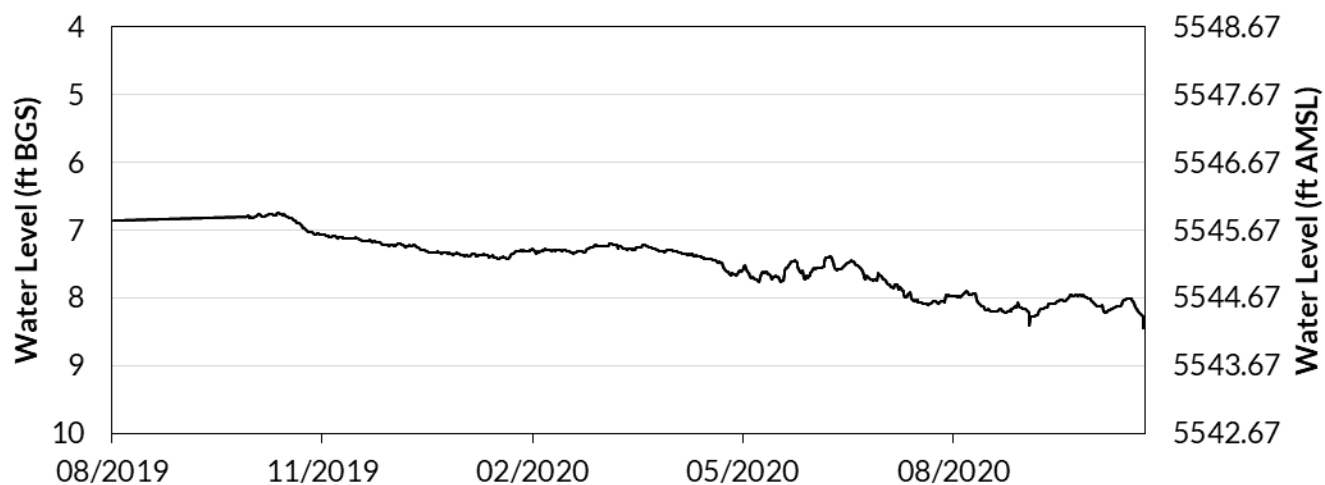
05N 26E 04BDD1



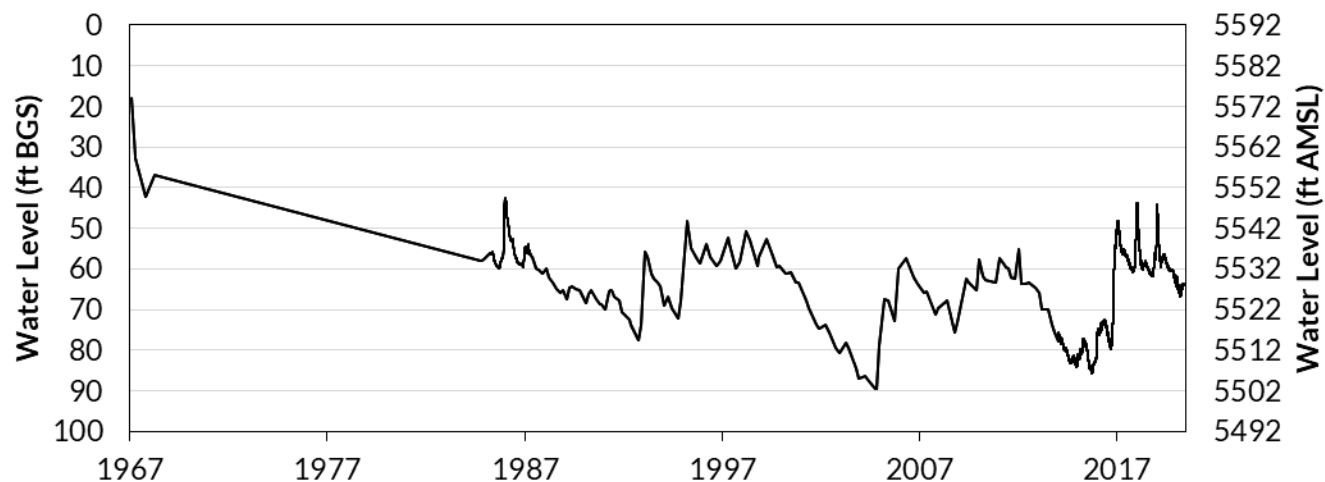
05N 26E 04BDD2



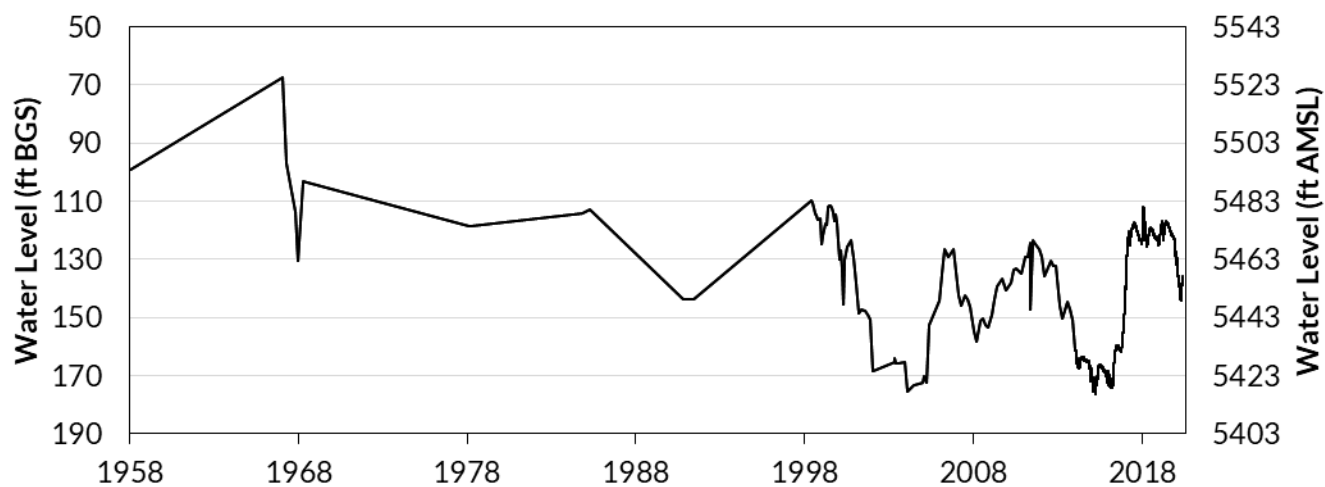
05N 26E 04BDD3



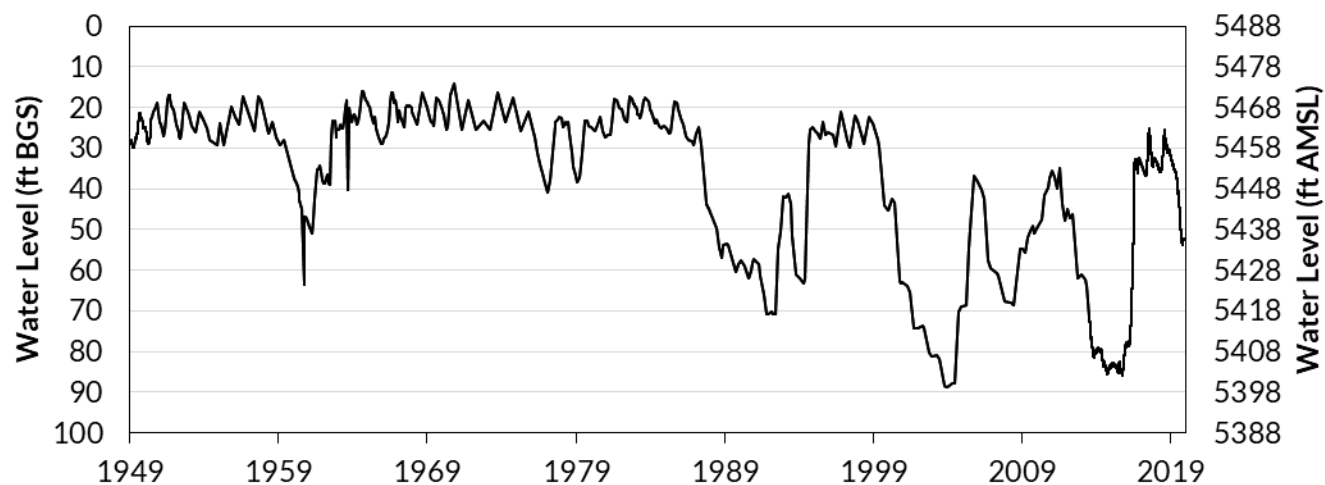
05N 26E 05DCB1



05N 26E 08CAB1



05N 26E 23CDA1

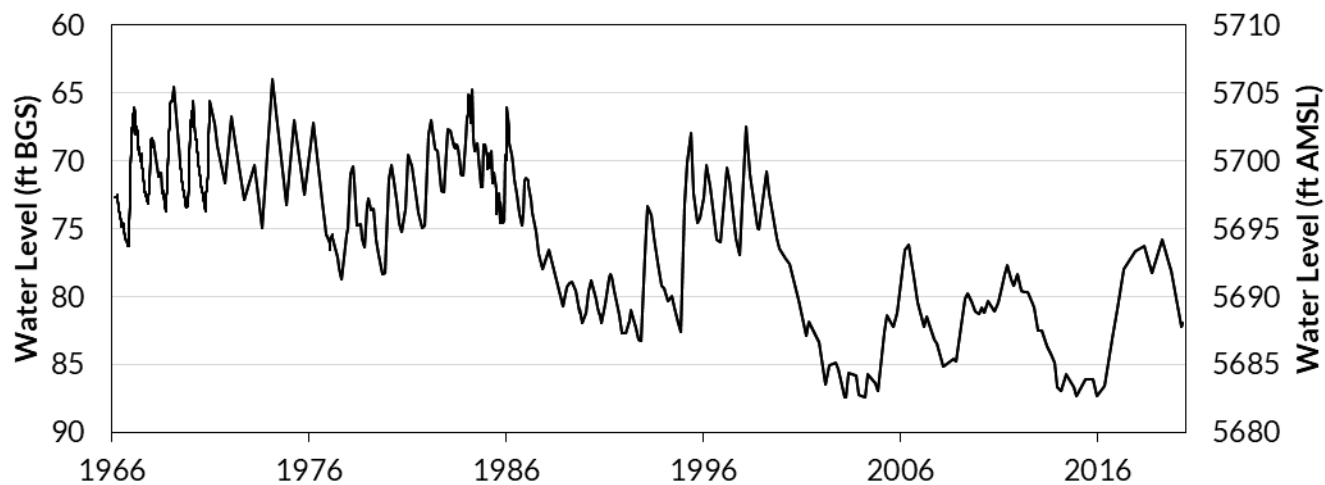


05N 26E 32DBA1

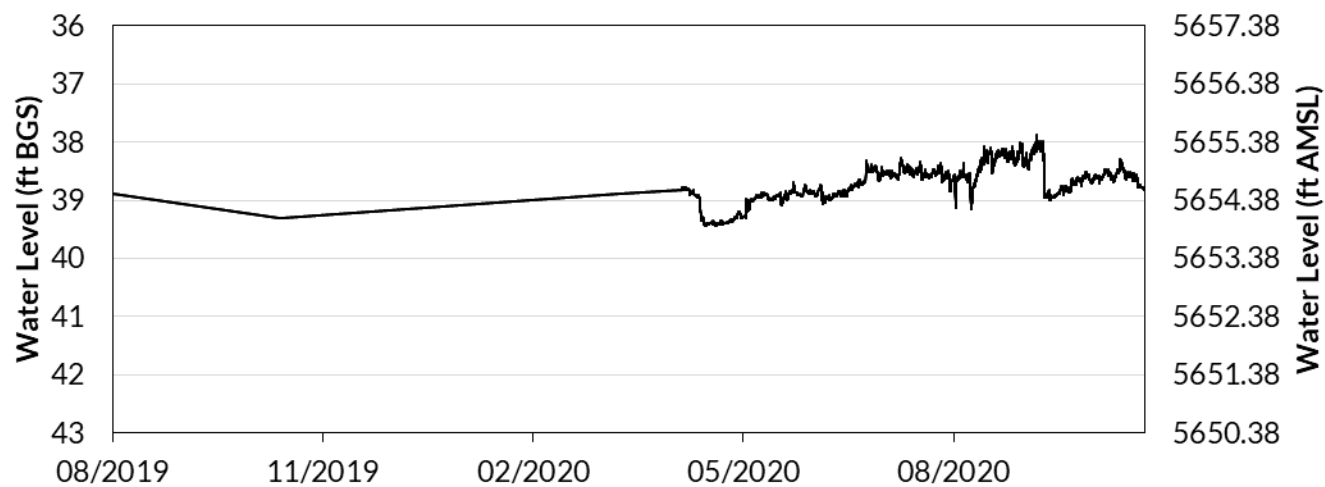




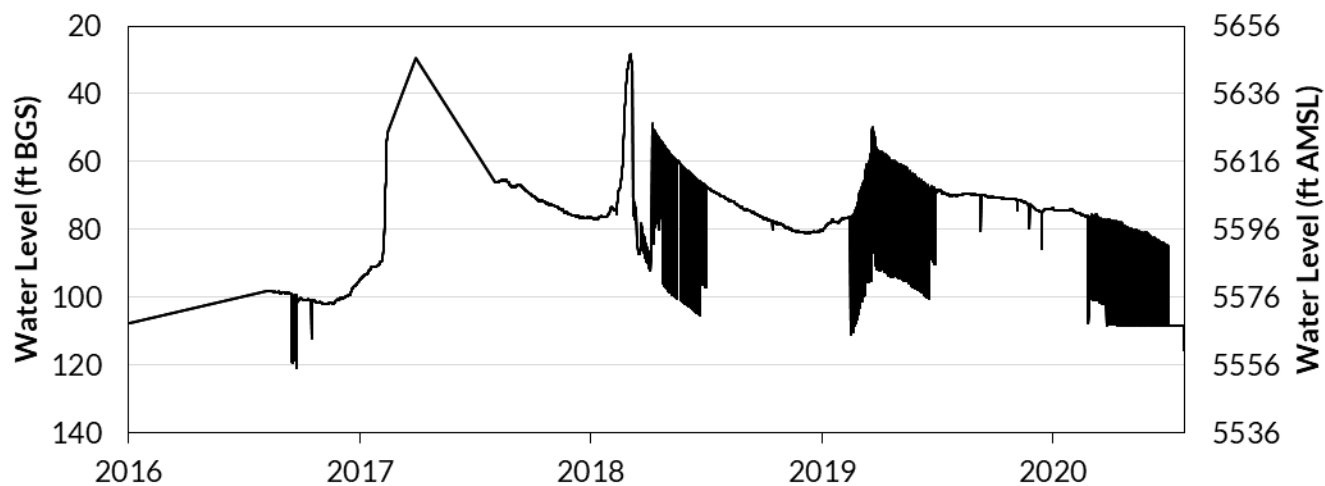
06N 25E 03AAA1



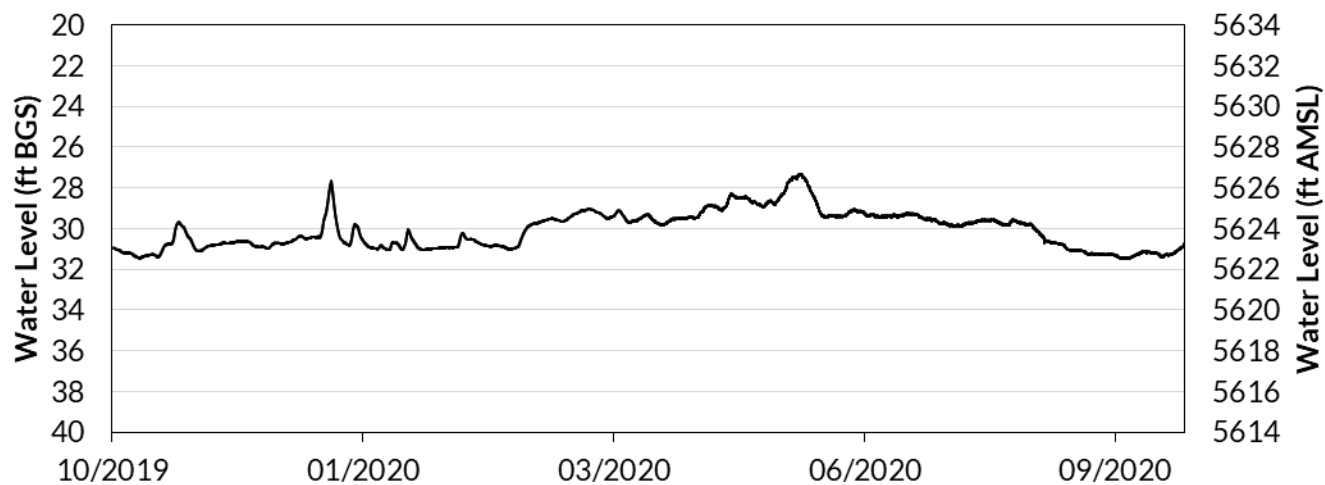
06N 25E 10CDA2



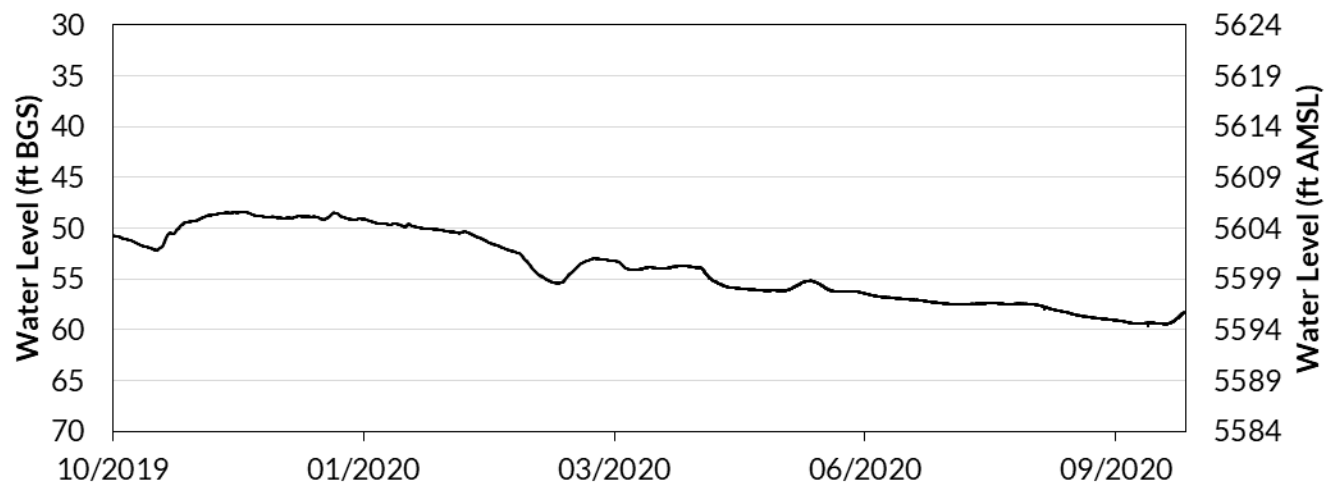
06N 25E 11CBC1



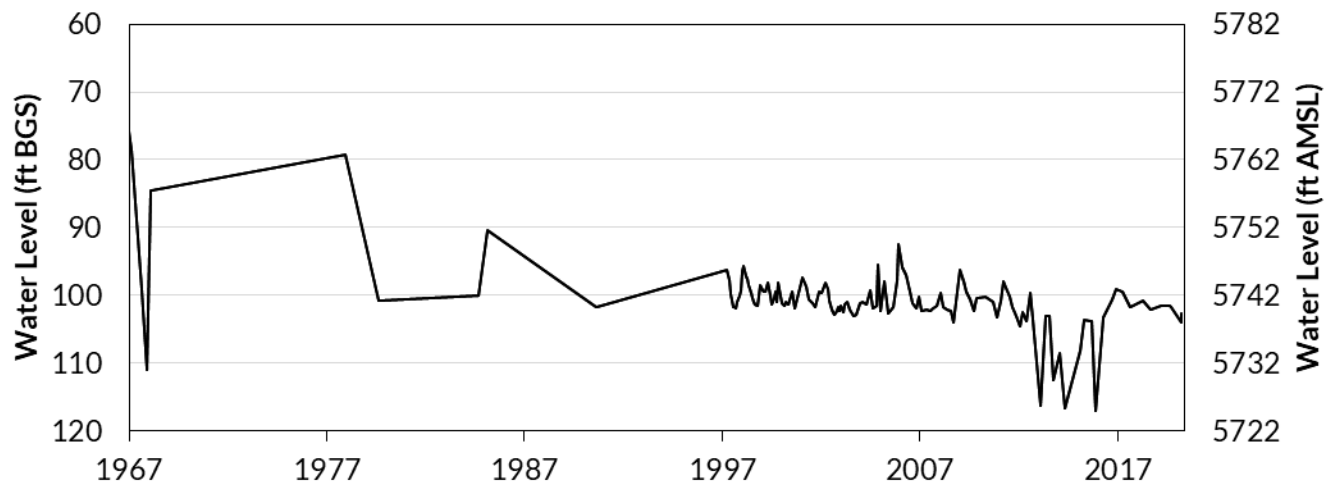
**06N 25E 14DAD2**

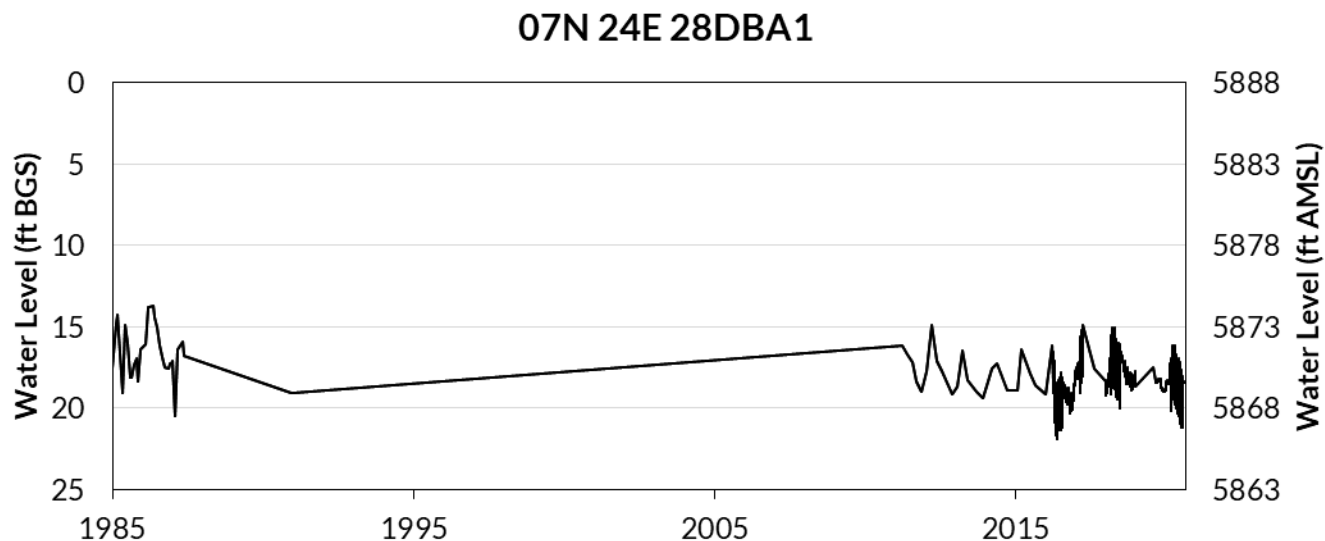
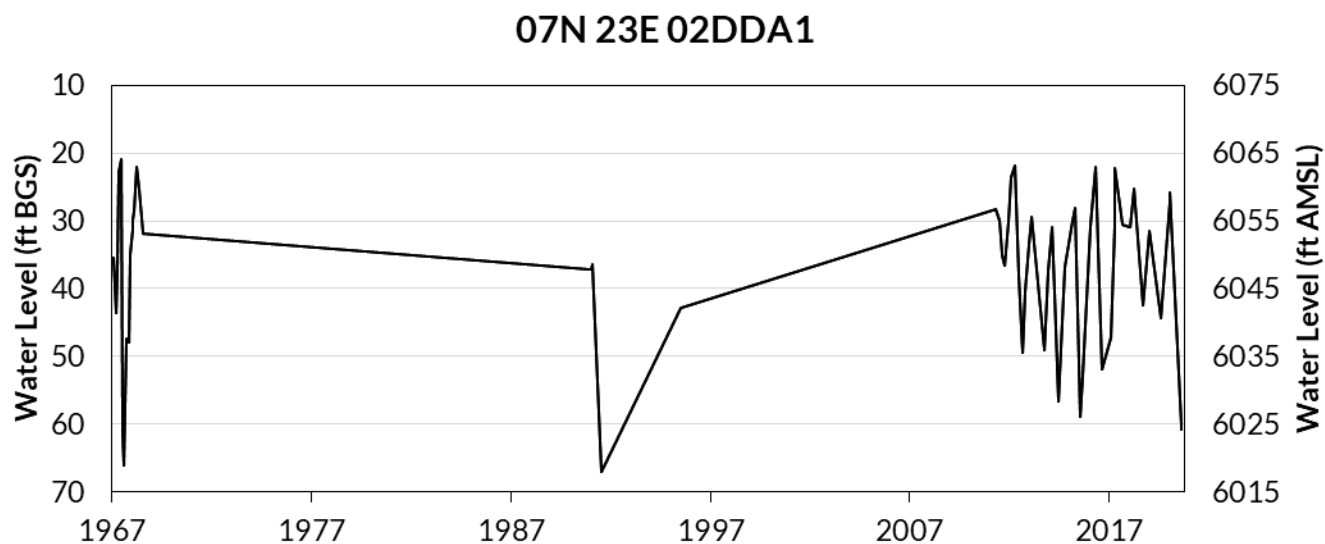
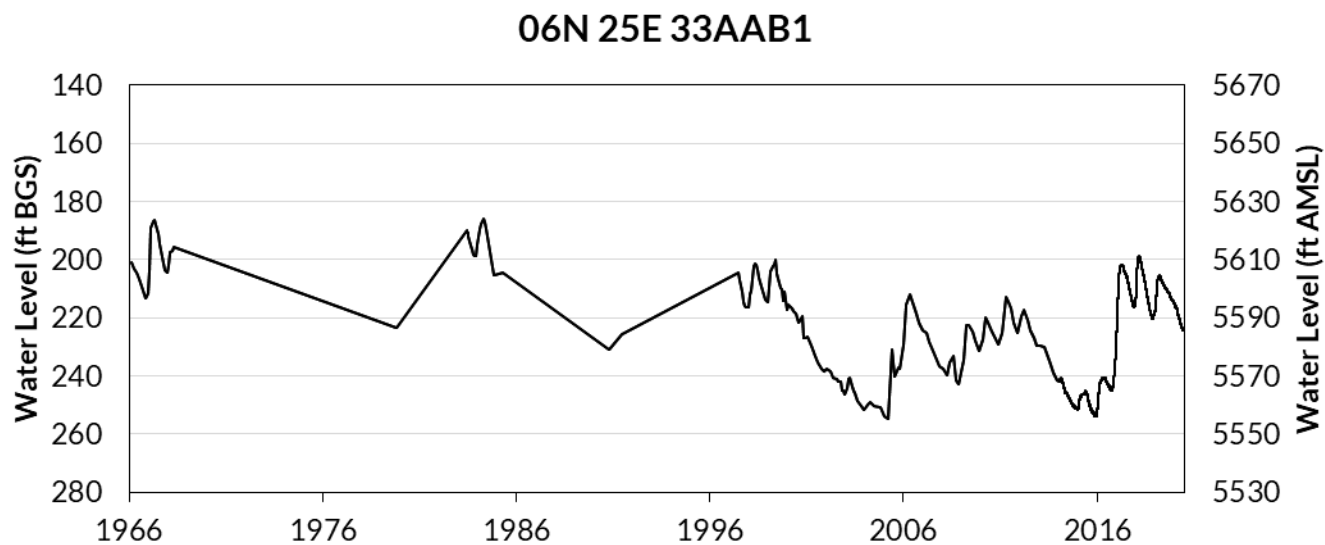


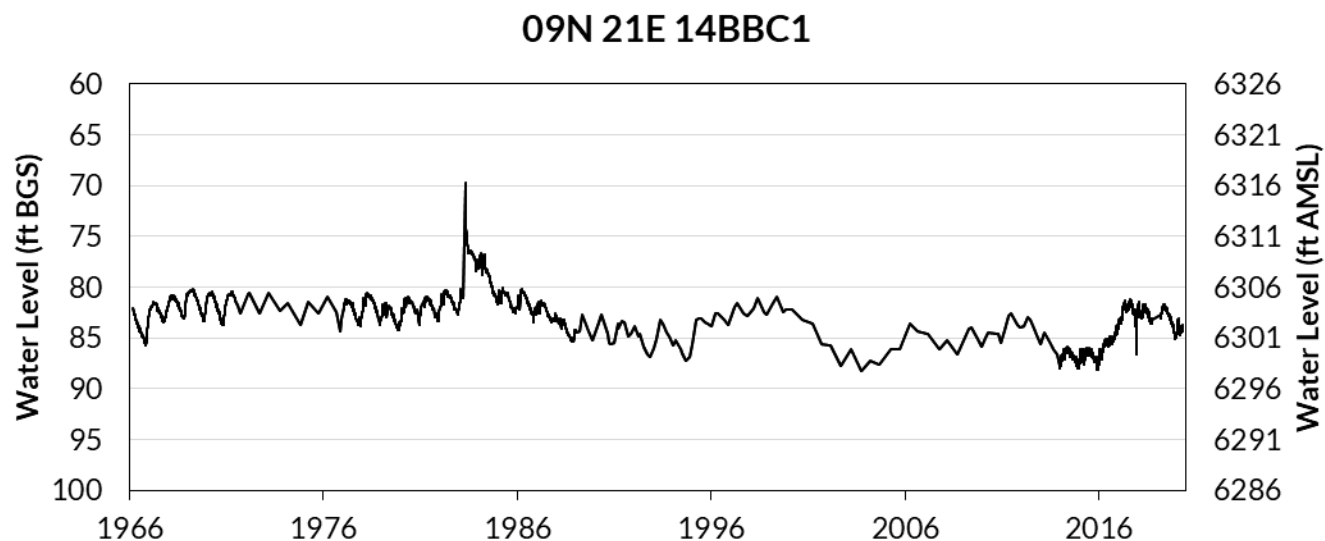
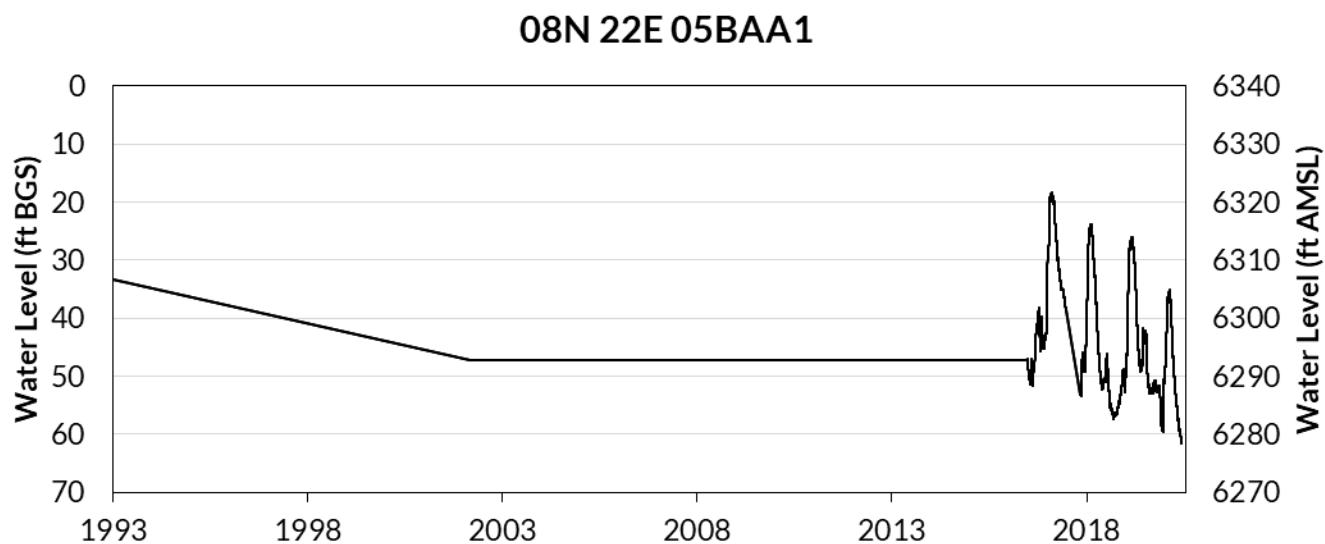
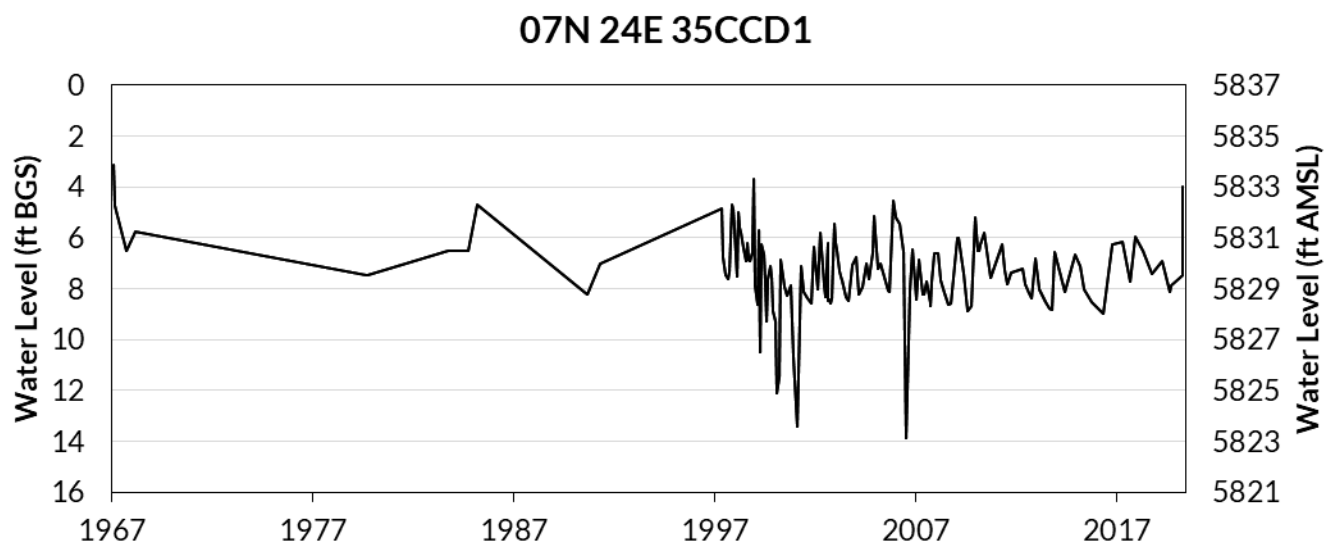
**06N 25E 14DAD3**



**06N 25E 18ABB1**







## Appendix B – Water Levels and Precipitation



**Table B.1:** Big Lost River Valley Network average optimal Pearson's R correlation coefficient for cumulative deviation from moving mean precipitation and ground water level variation. Correlations were higher when comparing to Copper Basin precipitation versus precipitation at individual well locations.

Well	Copper Basin Valley 108-month window	Individual Locations 120-month window
03N 27E 08BCB1	0.69	0.66
03N 27E 19AAB1	0.71	0.78
03N 27E 19ABB1	0.89	0.49
04N 26E 04BBA1	0.89	0.70
04N 26E 16ABB1	0.82	0.79
04N 26E 21ABB1	0.81	0.68
04N 26E 26DCD1	0.60	0.23
04N 26E 32CBB1	0.84	0.74
04N 27E 31DBC1	0.39	0.34
05N 25E 11BAA1	0.81	0.82
05N 26E 05DCB1	0.66	0.67
05N 26E 08CAB1	0.80	0.73
05N 26E 23CDA1	0.69	0.44
05N 26E 32DBA1	0.76	0.67
06N 25E 03AAA1	0.76	0.72
06N 25E 18ABB1	0.31	0.23
06N 25E 33AAB1	0.83	0.82
07N 23E 02DDA1	0.28	0.15
07N 24E 28DBA1	0.50	0.48
07N 24E 35CCD1	0.24	0.27
09N 21E 14BBC1	0.75	0.79
Mean Pearson's R	0.67	0.58

**Table B.2:** Big Lost River Valley Network Pearson's R correlation coefficient for cumulative deviation from moving mean precipitation, at Copper Basin and at each well, and ground water level variation at each well. Correlations were higher when comparing to Copper Basin precipitation versus precipitation at individual well locations.

Wells	Copper Basin Valley		Individual Locations	
	Mean Length (months)	PPT/GWL Pearson R	Mean Length (months)	PPT/GWL Pearson R
03N 27E 19ABB1	132	0.91	288	0.85
04N 26E 04BBA1	96	0.89	264	0.78
04N 26E 21ABB1	264	0.86	276	0.72
04N 26E 32CBB1	120	0.85	84	0.77
06N 25E 33AAB1	96	0.83	108	0.82
04N 26E 16ABB1	96	0.82	120	0.79
05N 25E 11BAA1	96	0.81	120	0.82
05N 26E 08CAB1	96	0.8	120	0.73
05N 26E 32DBA1	84	0.78	264	0.71
06N 25E 03AAA1	96	0.76	96	0.73
03N 27E 19AAB1	228	0.75	84	0.87
09N 21E 14BBC1	108	0.75	108	0.79
03N 27E 08BCB1	120	0.7	144	0.69
05N 26E 23CDA1	84	0.69	72	0.5
05N 26E 05DCB1	84	0.68	84	0.71
04N 26E 26DCD1	96	0.6	60	0.31
07N 24E 28DBA1	84	0.51	120	0.48
06N 25E 18ABB1	204	0.42	84	0.24
04N 27E 31DBC1	120	0.41	264	0.43
07N 24E 35CCD1	24	0.39	12	0.44
07N 23E 02DDA1	36	0.33	48	0.17
	Mean Pearson's R	0.69	Mean Pearson's R	0.64

## Appendix C – Mann-Kendall Test Results

**Table C.1:** Mann-Kendall Tests for fall depth to water measurements, Big Lost River Valley wells, entire record. Wells lacking sufficient data ( $n \geq 4$ ) were not included. Test results in bold represent a statistically significant trend,  $p < 0.05$ . A negative value indicates a rising water trend.

Well Number	slope (ft/yr)	Entire Record			
		tau	z	S	p
01S 22E 18DBD2	-0.30	-0.14	-0.69	-15	0.488
03N 26E 03DAA1	0.11	0.20	0.25	2	0.807
03N 27E 08BCB1	0.01	0.01	0.03	2	0.976
03N 27E 19AAB1	-0.36	-0.06	-0.10	-2	0.917
03N 27E 19ABB1	0.65	0.21	1.47	64	0.141
04N 26E 04BBA1	0.72	0.23	1.73	98	0.084
04N 26E 09BCA1	-6.45	-0.47	-1.13	-7	0.260
04N 26E 16ABB1	0.04	0.02	0.10	6	0.917
<b>04N 26E 21ABB1</b>	<b>0.70</b>	<b>0.53</b>	<b>5.64</b>	<b>736</b>	<b>0.000</b>
<b>04N 26E 26DCD1</b>	<b>0.30</b>	<b>0.48</b>	<b>5.96</b>	<b>1202</b>	<b>0.000</b>
<b>04N 26E 32CBB1</b>	<b>0.17</b>	<b>0.40</b>	<b>4.66</b>	<b>786</b>	<b>0.000</b>
<b>04N 27E 31DBC1</b>	<b>-0.76</b>	<b>-0.30</b>	<b>-2.01</b>	<b>-82</b>	<b>0.045</b>
05N 25E 11BAA1	-0.11	-0.01	-0.03	-2	0.976
<b>05N 26E 05DCB1</b>	<b>0.31</b>	<b>0.25</b>	<b>2.26</b>	<b>188</b>	<b>0.024</b>
05N 26E 08CAB1	0.43	0.13	0.88	41	0.378
<b>05N 26E 23CDA1</b>	<b>0.50</b>	<b>0.45</b>	<b>5.39</b>	<b>996</b>	<b>0.000</b>
05N 26E 32DBA1	0.37	0.05	0.30	14	0.761
<b>06N 25E 03AAA1</b>	<b>0.28</b>	<b>0.54</b>	<b>5.83</b>	<b>804</b>	<b>0.000</b>
06N 25E 11CBC1	3.08	0.20	0.25	2	0.807
<b>06N 25E 18ABB1</b>	<b>0.32</b>	<b>0.56</b>	<b>4.04</b>	<b>195</b>	<b>0.000</b>
<b>06N 25E 33AAB1</b>	<b>0.58</b>	<b>0.28</b>	<b>2.12</b>	<b>114</b>	<b>0.034</b>
07N 23E 02DDA1	1.00	0.11	0.41	7	0.680
07N 24E 28DBA1	0.04	0.23	1.10	21	0.272
07N 24E 35CCD1	0.04	0.26	1.94	99	0.053
08N 22E 05BAA1	4.15	0.80	1.72	8	0.086
<b>09N 21E 14BBC1</b>	<b>0.07</b>	<b>0.40</b>	<b>4.00</b>	<b>437</b>	<b>0.000</b>



**Table C.2:** Regional Mann-Kendall (RMK) Tests for fall depth to water measurements in Big Lost River Valley wells (below Mackay Dam), 1970-2020, 1970-1993, & 1993-2020. Test results from all three times periods represent statistically significant trends,  $p < 0.05$ . A negative value indicates a rising water trend.

	1970-2020					1990-2020					2010-2020				
	slope (ft/yr)	tau	z	S	p	slope (ft/yr)	tau	z	S	p	slope (ft/yr)	tau	z	S	p
Big Lost River Valley Network	0.38	0.478	10.62	2612	0.000	0.11	0.081	2.06	356	0.040	-0.40	-0.160	-2.91	-157	0.004

\*Due to limited historic data, the need for sufficient data (4+ fall measurements), and an attempt to maintain consistent measurement record for each well used in each RMK text, the three sets of RMK tests do not include exactly the same wells. The 1970-2020 RMK test included 5 wells, the 1990-2020 RMK test included 12 wells, and the 2010-2020 RMK test included 19 wells.

## Appendix D – Seasonal Water Level Changes

**Table D1:** Seasonal water level change in Big Lost River Valley wells. The negative sign indicates a deeper water level in fall vs. spring. For maximum and minimum fluctuation values, the absolute value of water level change was used in calculations.

Well Number	Period of Calculation	Maximum Spring-Fall Fluctuation (ft)	Minimum Spring-Fall Fluctuation (ft)	Average Spring-Fall Fluctuation (ft)
01S 22E 18DBD2	2005-2020	22.57	1.71	4.15
03N 25E 16ACC1	2019-2020	1.02	(-)0.33	0.35
03N 26E 03DAA1	1968-2020	(-)1.42	0.03	0.02
03N 26E 16ABB1*	2020	(-)0.5	(-)0.5	-0.5
03N 27E 06ACD1*	2020	(-)1.19	(-)1.19	-1.19
03N 27E 06ACD2*	2020	(-)0.98	(-)0.98	-0.98
03N 27E 06ACD3*	2020	(-)1.31	(-)1.31	-1.31
03N 27E 08BCB1	1967-2019	14.34	(-)0.46	0.81
03N 27E 19AAB1	1967-2020	19.58	(-)1.03	3.38
03N 27E 19ABB1	1985-2020	24.41	(-)0.26	1.32
04N 26E 04BBA1	1968-2020	36.35	2.51	-2.81
04N 26E 09BCA1	2015-2020	30.89	0.11	1.11
04N 26E 16ABB1	1968-2020	28.09	(-)0.14	-2.97
04N 26E 21ABB1	1971-2020	(-)9.78	(-)0.13	-0.59
04N 26E 21ABB2*	2020		Dry in Fall	
04N 26E 21ABB3*	2020	(-)20.83	(-)20.83	-20.83
04N 26E 21ABB4*	2020	(-)20.76	(-)20.76	-20.76
04N 26E 23CCC1*	2020	(-)11.25	(-)11.25	-11.25
04N 26E 23CCC2*	2020	(-)11.05	(-)11.05	-11.05
04N 26E 23CCC3*	2020	(-)10.28	(-)10.28	-10.28
04N 26E 26DCD1	1950-2020	20.17	(-)0.05	0.84
04N 26E 32CBB1	1961-2020	5.45	(-)0.03	0.51
04N 27E 31DBC1	1953-2020	14.34	(-)0.07	0.83
05N 25E 11BAA1	1968-2020	29.81	0.11	8.28
05N 26E 04BDD1*	2020	(-)0.74	(-)0.74	-0.74
05N 26E 04BDD2*	2020	(-)0.79	(-)0.79	-0.79
05N 26E 04BDD3*	2020	(-)1.16	(-)1.16	-1.16
05N 26E 05DCB1	1968-2020	21.88	0	2.97
05N 26E 08CAB1	1968-2020	35.77	0.18	-0.96
05N 26E 23CDA1	1950-2020	38.45	0.26	2.05
05N 26E 32DBA1	1985-2020	(-)41.67	0.98	-7.18
06N 25E 03AAA1	1967-2020	13.96	0.09	2.26

\*Newly added network wells with just one year of spring-fall measurements on record.

Table D1 continued.

Well Number	Period of Calculation	Maximum Spring-Fall Fluctuation (ft)	Minimum Spring-Fall Fluctuation (ft)	Average Spring-Fall Fluctuation (ft)
06N 25E 10CDA1*	2020		Dry Well	
06N 25E 10CDA2*	2020	0.06	0.06	0.06
06N 25E 10CDA3*	2020		Dry Well	
06N 25E 11CBC1	2016-2020	-40.94	5.29	2.24
06N 25E 14DAD1*	2020		Dry Well	
06N 25E 14DAD2*	2020	(-)1.17	(-)1.17	-1.17
06N 25E 14DAD3*	2020	(-)2.85	(-)2.85	-2.85
06N 25E 18ABB1	1968-2020	5.94	0.31	2.36
06N 25E 33AAB1	1967-2020	34.14	0.23	6.95
07N 23E 02DDA1	1967-2020	(-)34.98	(-)5.86	-16.90
07N 24E 28DBA1	1985-2020	1.44	0.01	0.41
07N 24E 35CCD1	1968-2020	3.89	0.12	0.82
08N 22E 05BAA1	2017-2020	(-)9.14	5.39	2.00
09N 21E 14BBC1	1967-2020	11.83	0.10	1.52
Overall average				-1.69
Average (excluding 1-year periods of calculation)				0.51